
THE CAUSAL IMPACT OF CREDIT LINES ON SPENDING DISTRIBUTIONS

Yijun Li^{*1}, Cheuk Hang Leung^{*1}, Xiangqian Sun², Chaoqun Wang¹, Yiyang Huang¹, Xing Yan³, Qi Wu^{†1}, Dongdong Wang⁴, and Zhixiang Huang⁴

¹School of Data Science, City University of Hong Kong

²Department of Financial and Actuarial Mathematics, Xi'an Jiaotong Liverpool University

³Institute of Statistics and Big Data, Renmin University of China

⁴JD Digits

ABSTRACT

Consumer credit services offered by e-commerce platforms provide customers with convenient loan access during shopping and have the potential to stimulate sales. To understand the causal impact of credit lines on spending, previous studies have employed causal estimators, based on direct regression (DR), inverse propensity weighting (IPW), and double machine learning (DML) to estimate the treatment effect. However, these estimators do not consider the notion that an individual's spending can be understood and represented as a distribution, which captures the range and pattern of amounts spent across different orders. By disregarding the outcome as a distribution, valuable insights embedded within the outcome distribution might be overlooked. This paper develops a distribution-valued estimator framework that extends existing real-valued DR-, IPW-, and DML-based estimators to distribution-valued estimators within Rubin's causal framework. We establish their consistency and apply them to a real dataset from a large e-commerce platform. Our findings reveal that credit lines positively influence spending across all quantiles; however, as credit lines increase, consumers allocate more to luxuries (higher quantiles) than necessities (lower quantiles). Our code is available at <https://github.com/lyjsilence/The-Causal-Impact-of-Credit-Lines-on-Spending-Distributions>.

1 Introduction

“Buy now, pay later” (BNPL) is a FinTech credit product offered by e-commerce platforms that allow consumers to make purchases first and defer payments later. BNPL is becoming increasingly popular due to its convenience in online shopping (Guttman-Kenney et al., 2023). In practice, e-commerce platforms assign different credit lines (the total amount of money that the platforms lends to a consumer) to potential customers according to their personal information and the history of purchases, payments, and default behaviors.

The primary goal of e-commerce platforms in introducing BNPL is to alter the consumption behavior of consumers, which is usually characterized as a specific *spending distribution* formed by the consumption

^{*}These authors contributed equally to this work.

[†]The corresponding author (qiwu55@cityu.edu.hk).

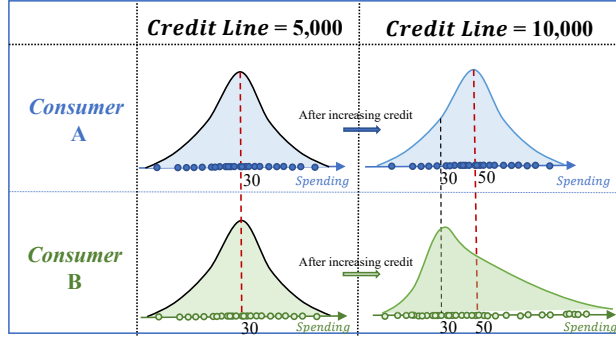


Figure 1: An example for the impact of credit lines change on spending distribution shift (one point stands for spending of one order).

amounts of the consumer’s all orders. The spending distributions of various consumers are different. For example, in Figure 7, the spending distribution of some consumers may exhibit a long tail, indicating a preference for both low-price necessities and high-price luxury items, whereas other consumers focus more on middle-valued products.

An essential question for e-commerce platforms is whether and how credit lines affect the consumption behavior of consumers. Previous studies have shown that increasing credit lines can lead to increased spending amounts, e.g., Aydin (2022); Soman and Cheema (2002). Nevertheless, they use a scalar quantity (e.g., *average spending* of all orders) to represent the spending of each consumer, which overlooks the complexity of consumption behaviors. For example, consider two consumers (A and B) in Figure 1. When the credit lines of them both equal 5,000, their spending distributions formed by 50 orders are the same, with an average spending of 30 dollars. Supposing the platform increases their credit lines to 10,000, consumer A prefers to increase the spending of all the orders by 20 dollars, and thus the shape of spending distribution does not change but parallelly shifts to the right by 20. On the other hand, consumer B prefers to purchase more luxury goods and remains the spending amounts of orders for necessities unchanged. The shape of consumer B’s spending distribution has shifted dramatically, but the average spending is the same as the first consumer (also increased from 30 to 50). Even though these two consumers have the same average spending, their spending behaviors are distinct after the change in credit lines. In this case, focusing only on the average spending loses some of the information of distribution (e.g., the part of quantile information). To this end, we propose to investigate *how the changes of credit lines affect the shift of spending distributions*. However, this raises another question: since classical causal inference literature targets the outcome of each individual as a scalar, *how can we perform causal inference when the outcome of each individual is a distribution?*

In this paper, we employ a novel causal framework to tackle this problem, where the outcome of each unit is a distribution, and the treatment takes multiple values. Based on Rubin’s causal framework (Rubin, 1977, 1978, 2005), we propose three estimators of target quantities: Direct Regression (DR) estimator, Inverse Propensity Weighting (IPW) estimator, and Doubly Machine Learning (DML) estimator. We first study the statistical asymptotic properties of these estimators. Then, to implement these estimators, we develop a deep-learning-based model named **Neural Functional Regression Net (NFR Net)** to estimate the complex relationship between functional output and scalar input. To assess the effectiveness of our methods, we conduct a simulation study. The results reveal that all three estimators are effective, especially for the DML estimator. We finally apply our approach to investigate the causal impact of credit lines on spending distributions based on a real-world dataset collected from a large e-commerce platform. We find that when credit lines increase, consumers’ spending tends to rise, which aligns with previous literature. Additionally, we reveal that the impact of credit lines is more significant in the high-quantile range of spending distribution,

suggesting that the increase in credit lines is associated with greater demands for luxury goods rather than necessities.

Our contributions can be summarized as follows:

- This is the first paper that explores the causal impact of credit lines on spending when the spending of each consumer is summarized as a distribution. Compared to the literature, we discover more detailed findings on the distribution quantiles.
- We consider the treatment takes multiple values, and we propose three estimators (i.e., DR, IPW, and DML estimators) for the target quantities. We study the statistical properties of these three estimators and compare them through a simulation experiment.
- The relation between functional output and scalar input is always non-linear and complex. Compared to existing works that captured it by a parameterized function or a linear function, we develop a deep learning model named NFR Net to learn this relationship.

2 Related Work

Causal inference is a significant challenge in various fields, such as finance (Huang et al., 2021) and health care (Shi et al., 2019). The key assumption of classical causal inference is that, given the treatment $D = d$, all the units have the same potential outcome distribution (unconditional). As a result, the realization of the outcome for each individual is a *scalar point* drawing from that potential outcome distribution (for instance, in Figure 2 when $D = d$, the blue (red) point is a realization of the i^{th} (j^{th}) unit). Under the assumption, several causal quantities are introduced and studied. For instance, the average treatment effect (ATE) (Chernozhukov et al., 2018) is the difference between the means of any two potential outcome distributions (i.e., $\mathbb{E}[Y(D = \bar{d})] - \mathbb{E}[Y(D = d)]$), or see the left half of Figure 2). Another quantity is the quantile treatment effect (QTE) (Chernozhukov and Hansen, 2005) that studies the difference between two potential outcome distributions at τ -quantiles (i.e., $Q(\tau, Y(D = \bar{d})) - Q(\tau, Y(D = d))$), or see the right half of Figure 2).

Various methods have been proposed to estimate the causal effect between treatment and outcome. A common approach is constructing the estimators for the target quantities. For example, Direct Regression (DR) incorporates all confounding factors into a single regression function. The inverse propensity weighting (IPW) method (Rosenbaum and Rubin, 1983; Hirano et al., 2003), on the other hand, assigns weights to the units based on their propensity scores which mimic RCTs in the pseudo population. However, both of them require accurate estimations of the nuisance parameters, such as the regression function and propensity scores. Doubly Machine Learning (DML) (Chernozhukov et al., 2018) method overcomes the shortcomings. It has the doubly robust property such that the accuracy of estimating nuisance parameters can be loosened.

The above methods are restricted when the outcome of each unit includes many observations or points and they constitute a *distribution*. For example, the shopping spending of a consumer may differ each time, and all the spending amounts form a distribution. In this case, it is impossible to infer the causal relationship via the standard framework unless we reduce the distributions to points (e.g., take the mean). Thus, it is necessary to seek alternative frameworks for distributional outcomes.

The distributional outcome can be treated as a continuous function. It is closely related to the field of functional data analysis that analyzes data under information varying over a continuum (Ramsay and Silverman, 2005; Wang et al., 2016; Cai et al., 2022; Chen et al., 2016). Jacobi et al. (2016) and Chib and Jacobi (2007) apply the functional data analysis to study the relationship between functional outcomes and independent variables based on the panel dataset. Nevertheless, they do not focus on the causal studying. Ecker et al.

(2023) considers a causal framework to study the impact of treatment on the functional outcome. However, their work conducts causal inference in Euclidean space. It is believed that the random structure of the distributional outcome is destroyed in the Euclidean space (Verdinelli and Wasserman, 2019; Panaretos and Zemel, 2019). As such, Lin et al. (2023) considers the causal study in the Wasserstein space, and we extend their framework to study the causal effect on distributional outcomes under multiple treatments and with a deep learning model NFR Net (statistical properties can be ensured as well). In this case, the realization of the outcome for each unit is a *distribution* (for example, in Figure 3 when $D = d$, the blue (red) distribution is a realization of the i^{th} (j^{th}) unit).

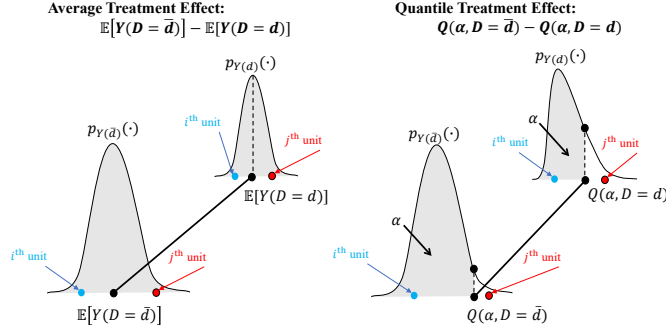


Figure 2: ATE and QTE in the literature.

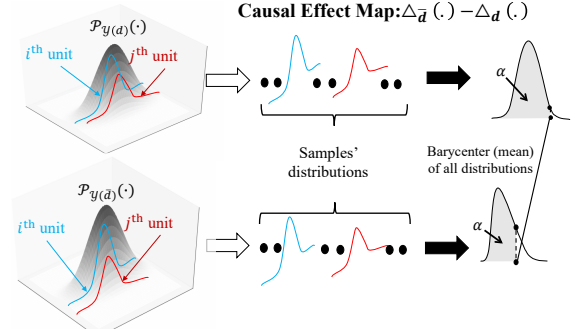


Figure 3: Causal Effect Map in our paper.

3 Causal Inference Framework

In this paper, we denote the *treatment* as D such that $D \in \mathcal{D} = \{d^1, \dots, d^r\}$, the *covariates/confounders* as $\mathbf{X} = [X^1, \dots, X^n] \in \mathcal{X}$, where \mathcal{X} is a bounded set in \mathbb{R}^n with distribution $F_{\mathbf{X}}$. With scalar outcomes, prior literature defines Y as the outcome variable and $Y(d)$ as the potential outcome variable when receiving treatment $D = d$. Note that $Y = \sum_{i=1}^r Y(d^i) \cdot \mathbf{1}_{\{D=d^i\}}$. Accordingly, the *potential outcome distribution and density* of $(Y, Y(d))$ is $(F_Y, F_{Y(d)})$ and $(P_Y, P_{Y(d)})$. In our framework, we consider the case where the outcome of each unit is a distribution that varies across units. To distinguish the differences, we use \mathcal{Y} as the outcome variable and $\mathcal{Y}(d)$ as the potential outcome variable when receiving treatment $D = d$. Similarly, $\mathcal{Y} = \sum_{i=1}^r \mathcal{Y}(d^i) \cdot \mathbf{1}_{\{D=d^i\}}$. We can then define the *potential outcome distribution and density* of $(\mathcal{Y}, \mathcal{Y}(d))$ as $(\mathcal{F}_{\mathcal{Y}}, \mathcal{F}_{\mathcal{Y}(d)})$ and $(\mathcal{P}_{\mathcal{Y}}, \mathcal{P}_{\mathcal{Y}(d)})$. We assume that there are N -independent units, i.e., $\{(D_s, \mathbf{X}_s, \mathcal{Y}_s)\}_{s=1}^N$.

3.1 Causal Assumptions

The following causal assumptions are standard under Rubin’s framework (Rubin, 2005): (1) *Consistency* (i.e., if $D = d^i$ occurs, then $\mathcal{Y} = \mathcal{Y}(d^i)$ a.s.); (2) *Ignorability/Unconfoundedness* (i.e., $\mathcal{Y}(d^i) \perp\!\!\!\perp D | \mathbf{X}, \forall i \in \{1, \dots, r\}$); (3) *Overlap* (i.e., $\mathbb{P}\{D = d^i | \mathbf{X}\} > 0, \forall i \in \{1, \dots, r\}$). We defer detailed explanations about the causal assumptions and the essentialness of each assumption to Appendix A.

3.2 Causal Quantities on Distributions

In our context, the realization of \mathcal{Y} for each unit is a distribution. It is inappropriate to conduct causal inference in the Euclidean space as it destroys the structure of distributions. For example, Figure 4 displays the distributions for 10 individual units (all are Gaussian distributions with different mean and variance), and the “mean” distribution of these 10 distributions obtained from Wasserstein metric (Barycenter) and Euclidean metric. We notice that the “mean” distribution cannot preserve the original Gaussian distribution structure unless the Wasserstein metric is used. We thus choose to conduct causal inference in the *Wasserstein*

Table 1: Comparisons between our framework and the framework given in the literature.

	Our framework	Literature framework
Treatment/Covariates variable	D/\mathbf{X}	D/\mathbf{X}
Outcome variable	$\mathcal{Y}, \mathcal{Y}(d)$	$Y, Y(d)$
Potential outcomes distribution (density)	$\mathcal{F}_{\mathcal{Y}(d)}(\cdot) (\mathcal{P}_{\mathcal{Y}(d)}(\cdot))$	$F_{Y(d)}(\cdot) (P_{Y(d)}(\cdot))$
Metric	Wasserstein	Euclidean
Space of outcome variable	$\mathcal{W}_2(\mathcal{I})$	$\mathcal{I} \in \mathbb{R}$
Realization of outcome variable	distribution	scalar
Target quantity	$\Delta_{d^i}, \Delta_{d^{ij}}$	$\mathbb{E}[Y(d^i)], \mathbb{E}[Y(d^j)] - \mathbb{E}[Y(d^j)]$

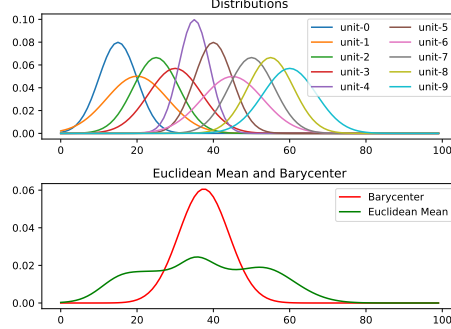


Figure 4: The Euclidean mean and Wasserstein mean (Barycenter) of 10 distributions.

space (Villani, 2021; Panaretos and Zemel, 2019; Feyeux et al., 2018). Here, we use the p -Wasserstein metric to characterize the “distance” between two distributions (see Definition 1). In the sequel, we let the realizations of $\mathcal{Y}, \mathcal{Y}(d)$ reside in \mathbb{R} .

Definition 1. Let $\mathcal{I} \subset \mathbb{R}$, $\mathcal{W}_p(\mathcal{I}) = \{\lambda : \int_{\mathcal{I}} s^p d\lambda(s) < \infty\}$ (λ is a distribution), and $\Lambda(\lambda_1, \lambda_2)$ be the set containing the joint distribution $\Pi(\lambda_1(s), \lambda_2(t))$ whose marginals are λ_1 and λ_2 . The p -Wasserstein metric between two distributions λ_1 and λ_2 is

$$\mathbb{D}_p(\lambda_1, \lambda_2) = \left\{ \inf_{\Pi \in \Lambda(\lambda_1, \lambda_2)} \int_{\mathcal{I}} |s - t|^p d\Pi(\lambda_1(s), \lambda_2(t)) \right\}^{\frac{1}{p}}.$$

$\mathbb{D}_p(\cdot, \cdot)$ satisfies the axioms of a metric (i.e., non-negativity, symmetric, and triangle inequality). Usually, we set $p = 2$. Next, we introduce two quantities - the causal map and the causal effect map.

Definition 2. The causal map of treatment d^i is denoted as $\Delta_{d^i}^\dagger$ such that

$$\Delta_{d^i} = \mu_{d^i}^{-1}, \quad (1)$$

where $\mu_{d^i} = \arg \min_{v \in \mathcal{W}_2(\mathcal{I})} \mathbb{E}[\mathbb{D}_2(\mathcal{Y}(d^i), v)^2]$ is the Wasserstein barycenter/mean of units’ distributions when they take the treatment d^i . The superscript “ -1 ” of μ_{d^i} is the inverse of the cumulative distribution function (CDF) or the quantile function. Hence, the causal effect map between treatment d^i and d^j is

$$\Delta_{d^{ij}} = \Delta_{d^i} - \Delta_{d^j} = \mu_{d^i}^{-1} - \mu_{d^j}^{-1}. \quad (2)$$

The causal effect map in Eqn. (2) is an analogy to the ATE ($\mathbb{E}[Y(d^i)] - \mathbb{E}[Y(d^j)]$) in the literature. However, $\Delta_{d^i}, \Delta_{d^j}$ and $\Delta_{d^{ij}}$ are functions, but $\mathbb{E}[Y(d^i)], \mathbb{E}[Y(d^j)],$ and $\mathbb{E}[Y(d^i)] - \mathbb{E}[Y(d^j)]$ are scalars. In Table 1, we summarize the differences between the framework in our paper and in the literature.

[†] Δ_{d^i} is a function and should be $\Delta_{d^i}(\cdot)$ formally. In the sequel, we use both Δ_{d^i} and $\Delta_{d^i}(\cdot)$ interchangeably.

Remark 1.

1. Classically, the case “distribution over \mathbb{R} ” means that a realization is a point (scalar or vector) drawing from the distribution of the potential outcome, while the case “distribution over distributions” means that the realization is a distribution. For instance, let μ and σ be the mean and standard deviation of a normal distribution, and $(\mu, \log \sigma) \sim \mathcal{N}(\mathbf{0}, \mathbb{I}_2)$. If the realization $(\mu, \log \sigma)$ of a unit (e.g., a consumer) is $(0.1, -0.5)$, then it means that a collection of observations (e.g., spending amounts of all orders) are drawn from $\mathcal{N}(0.1, e^{-1})$ for this unit.
2. $\Delta_{d^i}(\cdot)$ is a quantile function (inverse of CDF), so does $\Delta_{d^j}(\cdot)$. Further, we can explore the impact of between treatment d^i and d^j on the distributional outcome respectively at a specific τ quantile level by $\Delta_{d^{ij}}(\cdot)$, i.e.,

$$\Delta_{d^{ij}}(\tau) = \Delta_{d^i}(\tau) - \Delta_{d^j}(\tau) = \mu_{d^i}^{-1}(\tau) - \mu_{d^j}^{-1}(\tau). \quad (3)$$

Note that $\Delta_{d^{ij}}(\tau)$ differs from the quantile treatment effect (QTE) in the literature (e.g., Machado and Mata (2005); Chernozhukov and Hansen (2005)). $\Delta_{d^{ij}}(\tau)$ is the τ -quantiles difference of the **barycenters** under treatments d^i and d^j , but QTE is the τ -quantiles difference of the **potential outcome distributions** under two treatments. It is thus inappropriate to compare them or study $\Delta_{d^{ij}}(\tau)$ using the approaches in the QTE literature. The visualized difference of the two quantities is given in Figure 2 and 3.

We need to ensure Δ_{d^i} is *identifiable* such that we can estimate it from an observed dataset. It is also necessary to simplify the calculation of μ_{d^i} to address the computational complexity of optimal transport. Proposition 1 states an equivalent form of Δ_{d^i} without computing optimization and guarantees that we can estimate it from the observed dataset:

Proposition 1. *Given the conditions in Definition 1 and 2, and Assumptions (1) - (3) hold, we have (1) $\Delta_{d^i} = \mathbb{E}[\mathcal{Y}(d^i)^{-1}]$; (2) Δ_{d^i} is identifiable.*

The first assertion gives a simpler way to compute Δ_{d^i} , while the second assertion ensures that Δ_{d^i} is identifiable. We defer the proofs to Appendix D.

3.3 Estimators

Similar to the causal inference methods in the literature (Horvitz and Thompson, 1952; Chernozhukov et al., 2018), we also propose three estimators to compute the causal map Δ_{d^i} , namely (1) *Direct Regression (DR) estimator* ($\Delta_{d^i;DR}$), (2) *Inverse Probability Weighting (IPW) estimator* ($\Delta_{d^i;IPW}$), and (3) *Double Machine Learning (DML) estimator* ($\Delta_{d^i;DML}$). Let $\pi_{d^i}(\mathbf{X}) = \mathbb{P}\{D = d^i | \mathbf{X}\}$ and $m_{d^i}(\mathbf{X}) = \mathbb{E}[\mathcal{Y}^{-1} | D = d^i, \mathbf{X}]$. Given that there are N units. The estimators are:

$$\Delta_{d^i;DR} = \frac{1}{n} \sum_{s=1}^n m_{d^i}(\mathbf{X}_s) \quad (4)$$

$$\Delta_{d^i;IPW} = \frac{1}{n} \sum_{s=1}^n \frac{\mathbf{1}_{\{D_s=d^i\}}}{\pi_{d^i}(\mathbf{X}_s)} (\mathcal{Y}_s^{-1}) \quad (5)$$

$$\Delta_{d^i;DML} = \frac{1}{n} \sum_{s=1}^n \left[m_{d^i}(\mathbf{X}_s) + \frac{\mathbf{1}_{\{D_s=d^i\}}}{\pi_{d^i}(\mathbf{X}_s)} (\mathcal{Y}_s^{-1} - m_{d^i}(\mathbf{X}_s)) \right]. \quad (6)$$

3.4 Theory and Algorithm

In practical scenarios, when using all the available units to train the regression function $m_{d^i}(\mathbf{X}_s)$ and propensity score function $\pi_{d^i}(\mathbf{X}_s)$, there is a risk of over-fitting. To mitigate this issue, a cross-fitting

technique, as introduced by Chernozhukov et al. (2018), is commonly employed. Along this way, we also need to obtain the cross-fitting estimators of Δ_{d^i} according to Eqns. (4), (5), and (6).

We split the N units into K disjoint groups. Let the k^{th} group be \mathcal{D}_k of size N_k , $\forall k = 1, \dots, K$. Denoting $\mathcal{D}_{-k} = \cup_{r=1, r \neq k}^K \mathcal{D}_r$, we use \mathcal{D}_{-k} to obtain $\hat{m}_{d^i}^k(\mathbf{X})$, $\hat{\pi}_{d^i}^k(\mathbf{X})$, which are the estimations of $m_{d^i}^k(\mathbf{X})$, $\pi_{d^i}^k(\mathbf{X})$ for the k^{th} group. $\hat{\mathcal{Y}}$ is the empirical estimation of \mathcal{Y} . We then use \mathcal{D}_k to compute the estimation of $\Delta_{d^i}^k$ (i.e., $\hat{\Delta}_{d^i;DR}^k$, $\hat{\Delta}_{d^i;IPW}^k$, and $\hat{\Delta}_{d^i;DML}^k$) according to Eqns. (7), (8), and (9) respectively. We thus define $\hat{\Delta}_{d^i;DR}^k$, $\hat{\Delta}_{d^i;IPW}^k$, and $\hat{\Delta}_{d^i;DML}^k$ such that

$$\hat{\Delta}_{d^i;DR}^k = \frac{1}{N_k} \sum_{s \in \mathcal{D}_k} \hat{m}_{d^i}^k(\mathbf{X}_s) \quad (7)$$

$$\hat{\Delta}_{d^i;IPW}^k = \frac{1}{N_k} \sum_{s \in \mathcal{D}_k} \frac{\mathbf{1}_{\{D_s=d^i\}}}{\hat{\pi}_{d^i}^k(\mathbf{X}_s)} \hat{\mathcal{Y}}_s^{-1} \quad (8)$$

$$\hat{\Delta}_{d^i;DML}^k = \frac{1}{N_k} \sum_{s \in \mathcal{D}_k} \left[\hat{m}_{d^i}^k(\mathbf{X}_s) + \frac{\mathbf{1}_{\{D_s=d^i\}}}{\hat{\pi}_{d^i}^k(\mathbf{X}_s)} (\hat{\mathcal{Y}}_s^{-1} - \hat{m}_{d^i}^k(\mathbf{X}_s)) \right]. \quad (9)$$

Denoting $w \in \{DR, IPW, DML\}$, the cross-fitting estimators are $\hat{\Delta}_{d^i;w}$ such that

$$\hat{\Delta}_{d^i;w} = \sum_{k=1}^K \frac{N_k}{N} \hat{\Delta}_{d^i;w}^k. \quad (10)$$

We study the consistency of $\hat{\Delta}_{d^i;w}$. When $w = DR$ or IPW , the results are deferred to Appendix C. When $w = DML$, the consistency result is given in Theorem 1 while the proofs and the notational meanings are deferred to Appendix D.

Theorem 1. *Let $\tilde{m}_{d^i}^k(\mathbf{X})$ ($\hat{m}_{d^i}^k(\mathbf{X})$) be the estimate of $\mathbb{E}[\mathcal{Y}^{-1}|D = d^i, \mathbf{X}]$ using the true \mathcal{Y} (estimated $\hat{\mathcal{Y}}$) based on \mathcal{D}_{-k} . Suppose that, for any k , $\rho_\pi^4 = \mathbb{E}[|\hat{\pi}_{d^i}^k(\mathbf{X}) - \pi_{d^i}(\mathbf{X})|^4]$, $\rho_m^4 = \max\{\|\tilde{m}_{d^i}^k - m_{d^i}\|^4, 1 \leq i \leq r\} = \max\{[\int \|\tilde{m}_{d^i}^k(\mathbf{x}) - m_{d^i}(\mathbf{x})\|^2 dF_{\mathbf{X}}(\mathbf{x})]^2, 1 \leq i \leq r\}$. Under the convergence assumptions in Appendix D, we have*

1. $\|\hat{\Delta}_{d^i;DML} - \Delta_{d^i}\| = O_P(N^{-\frac{1}{2}} + N^{-\frac{1}{2}}\rho_\pi + N^{-\frac{1}{2}}\rho_m + \rho_\pi\rho_m)$.
2. *If $\rho_m\rho_\pi = o(N^{-\frac{1}{2}})$, $\rho_m = o(1)$ and $\rho_\pi = o(1)$, then $\sqrt{N}(\hat{\Delta}_{d^i;DML} - \Delta_{d^i})$ converges weakly to a centred Gaussian process.*

Theorem 1 not only gives the consistency of $\hat{\Delta}_{d^i;DML}$, but also gives the convergence speed of $\hat{\Delta}_{d^i;DML}$. It is indeed a \sqrt{N} -consistent estimator.

We can also investigate the \sqrt{N} -consistency of the DR or IPW estimators. In fact, we can obtain the desired results by setting $\mathbf{1}_{\{D=d^i\}} = 0$ and $(m_{d^i}, \hat{m}_{d^i}^k, \tilde{m}_{d^i}^k) = (0, 0, 0)$ in the proofs of Theorem 1 respectively. Last but not least, we summarize the steps of computing $\hat{\Delta}_{d^i;w}$ in Algorithm 1.

3.5 Models

To estimate the target quantity Δ_{d^i} , we need to estimate several nuisance parameters accurately, e.g., \mathcal{Y}^{-1} , $\pi_{d^i}(\mathbf{X})$, and $m_{d^i}(\mathbf{X})$. First, to estimate \mathcal{Y}^{-1} , we can estimate \mathcal{Y} empirically and invert the estimated \mathcal{Y} (CDF) for each unit to get the $\hat{\mathcal{Y}}^{-1}$. Second, $\pi_{d^i}(\mathbf{X})$ is the *propensity score* that can be estimated using the multi-class logistic regression, random forest classifier, or feed-forward networks. Finally, we can estimate

Algorithm 1 Computations of $\hat{\Delta}_{d^i;w}$

Require: The observations of $(D_s, \mathbf{X}_s, \mathcal{Y}_s)_{s=1}^N$.

Ensure: $\hat{\Delta}_{d^i;w}$ for $w \in \{DR, IPW, DML\}$.

- 1: Split $(D_s, \mathbf{X}_s, \mathcal{Y}_s)_{s=1}^N$ to K disjoint units groups \mathcal{D}_k of size N_k and form \mathcal{D}_{-k} .
- 2: Estimate $\hat{\mathcal{Y}}_s^{-1}$ for each unit s .
- 3: **for** $k \leftarrow 1$ to K **do**
- 4: Regress D w.r.t. \mathbf{X} based on \mathcal{D}_{-k} and obtain $\hat{\pi}_{d^i}^k$.
- 5: Regress $\hat{\mathcal{Y}}_s^{-1}$ w.r.t. (D, \mathbf{X}) based on \mathcal{D}_{-k} and obtain $\hat{\eta}_{d^i}^k$.
- 6: Compute $\hat{\Delta}_{d^i;w}^k$ using Eqns. (7), (8) and (9) according to w .
- 7: **end for**
- 8: Compute $\hat{\Delta}_{d^i;w}$ using Eqn. (10).

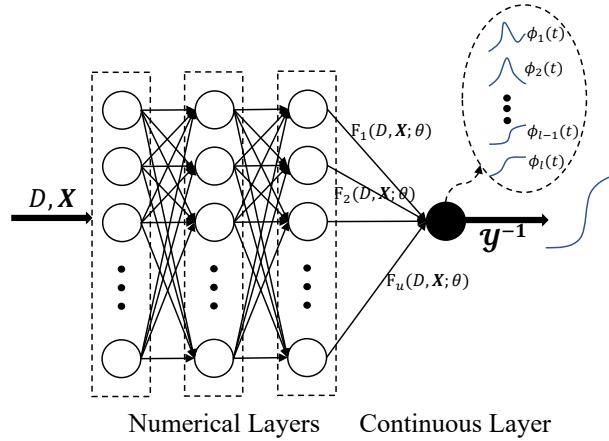


Figure 5: The proposed NFR Net.

the regression function $m_{d^i}(\mathbf{X})$ by regressing the outcome \mathcal{Y}^{-1} on treatment D and covariates \mathbf{X} via a *functional-on-scalar regression*. The first two quantities can be well estimated using the classical approaches. On the other hand, the third quantity, $m_{d^i}(\mathbf{X})$, is difficult to estimate accurately using the classical functional regression approach. Specifically, the classical functional regression (Ramsay and Silverman, 2005) assumes that the regression equation between outcome \mathcal{Y}^{-1} and predictors (D, \mathbf{X}) can be approximated by a finite series of some pre-determined basis functions, i.e.,

$$\mathcal{Y}^{-1}(t) = D \sum_{l=1}^v \gamma_{0l} \phi_l(t) + \sum_{j=1}^n X^j \left(\sum_{l=1}^v \gamma_{jl} \phi_l(t) \right) + \epsilon(t), \quad (11)$$

where $\mathcal{Y}^{-1}(t)$ is the response function; $(D, \mathbf{X}) = [D, X^1, \dots, X^j, \dots, X^n]$ are predictors; $\{\phi_1, \dots, \phi_v\}$ are basis functions, e.g., B-spline basis; γ_{jl} with $0 \leq j \leq n$ and $1 \leq l \leq v$ are regression parameters; and $\epsilon(t)$ is the noise term.

However, the relation between $\mathcal{Y}^{-1}(t)$ and (D, \mathbf{X}) may not be additive as in Eqn. (11). Generally, the relationship is non-linear and complex. To this end, we design **Neural Functional Regression (NFR) Net** to address this issue. The NFR Net consists of two parts: (1) the *numerical layers*, and (2) the *continuous layer* (see Figure 5). Under our framework and settings, the numerical layers aim to learn the u representations $F(D, \mathbf{X}; \theta) = [F_1(D, \mathbf{X}; \theta), \dots, F_u(D, \mathbf{X}; \theta)]^\top$, where each $F_i(D, \mathbf{X}; \theta)$, $1 \leq i \leq u$ is a linear coefficient to constitute the target distribution. The representations $F(D, \mathbf{X}; \theta)$ is then processed by a continuous layer

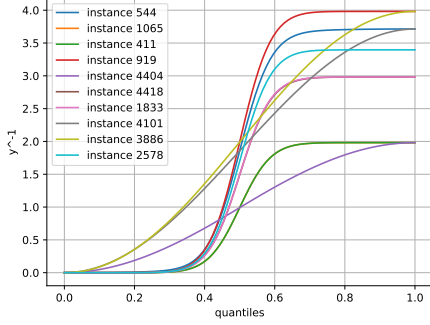
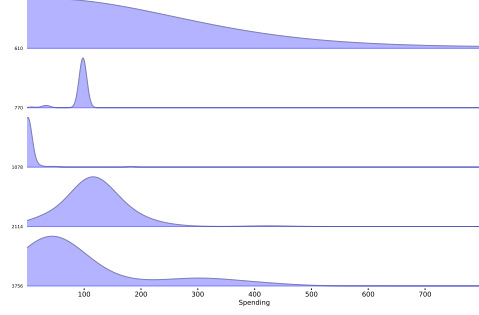

 Figure 6: 10 instances of simulated quantile function (\mathcal{Y}^{-1}).


Figure 7: The spending distribution of 5 consumers from a e-commerce platform.

to output a function $\tilde{\mathcal{Y}}^{-1}$, i.e.,

$$\tilde{\mathcal{Y}}^{-1}(t; \theta, \{\gamma_{ij}\}) = \sum_{i=1}^u F_i(D, \mathbf{X}; \theta) \sum_{j=1}^v \gamma_{ij} \phi_j(t), \quad (12)$$

where $\{\gamma_{ij}\}$ now are trainable parameters and $\{\phi_j(t)\}$ are pre-defined basis functions.

The model can be trained as follows: let L be the loss metric (e.g., L_1 or L_2 loss), and our task is equivalent to finding the optimal $\theta, \{\gamma_{ij}\}$ by minimizing the loss function $\mathcal{L}(\theta, \{\gamma_{ij}\})$:

$$\min_{\theta, \{\gamma_{ij}\}} \mathcal{L}(\theta, \{\gamma_{ij}\}) := \int L(\tilde{\mathcal{Y}}^{-1}(t; \theta, \{\gamma_{ij}\}), \hat{\mathcal{Y}}^{-1}(t)) dt. \quad (13)$$

In practice, we can estimate the integral using the trapezoidal rule/Simpson's rule by taking any number of discrete quantile points t .

4 Synthetic Experiment

Data Generation Process Since the ground truth is unavailable in the real dataset, we simulate data using the following data generation process for the s^{th} unit to test our proposed model similar to many other causal inference studies:

$$\mathcal{Y}_s^{-1}(D_s) = c + (1 - c)(\mathbb{E}[D] + \sqrt{D_s}) \times \sum_{j=1}^{\frac{n}{2}} \frac{\exp(X_s^{2j-1} X_s^{2j})}{\sum_{k=1}^{\frac{n}{2}} \exp(X_s^{2k-1} X_s^{2k})} \mathbf{B}^{-1}(\alpha_j, \beta_j) + \epsilon_s, \quad (14a)$$

$$\mathbb{P}\{D_s = d \mid \mathbf{X}_s\} = \frac{\exp(\gamma_d^\top \mathbf{X}_s)}{\sum_{w=1}^r \exp(\gamma_w^\top \mathbf{X}_s)}. \quad (14b)$$

In our experiment, we set $n = 10$. We assume that covariates $X^1, X^2 \sim \mathcal{N}(-2, 1)$, $X^3, X^4 \sim \mathcal{N}(-1, 1)$, $X^5, X^6 \sim \mathcal{N}(0, 1)$, $X^7, X^8 \sim \mathcal{N}(1, 1)$, $X^9, X^{10} \sim \mathcal{N}(2, 1)$, and $\epsilon_s \sim \mathcal{N}(0, 0.05)$. $\mathbf{B}^{-1}(\alpha, \beta)$ is the inverse CDF of Beta distribution with the shape parameters α and β . We select 5 inverse Beta CDFs, where each one has different parameters to ensure the complexity of the distribution function. The treatment D takes the value in $\{d^1, d^2, d^3, d^4, d^5\}$ with a softmax distribution. $c \in [0, 1]$ is the constant that controls the strength of the causal relationship between treatment D and outcome distribution \mathcal{Y}^{-1} . In one experiment, 5,000 instances are generated according to Eqns. (14a) - (14b). For each unit s , 100 observations are sampled from the inverse CDF using the inverse transform sampling method. Figure 6 summarizes 10 simulated instances, indicating that the inverse CDF of each instance varies widely.

Table 2: MAE between true and estimated causal effect maps under various methods of regressing $\hat{\mathcal{Y}}^{-1}$ w.r.t. (D, \mathbf{X}) (mean \pm standard deviation with 100 trials). Best results are in bold.

	Q=10%	Q=30%	Q=50%	Q=70%	Q=90%	Average
DR						
Lasso	0.066	0.064	0.121	0.183	0.184	0.124 \pm 0.053
Ridge	0.066	0.075	0.093	0.167	0.189	0.118 \pm 0.050
Elastic net	0.066	0.064	0.121	0.183	0.184	0.124 \pm 0.053
MCP	0.066	0.075	0.093	0.167	0.189	0.118 \pm 0.050
D/DML	0.010	0.058	0.299	0.517	0.615	0.300 \pm 0.240
NFR	0.025	0.104	0.039	0.053	0.040	0.052 \pm 0.027
IPW						
Lasso	0.010	0.061	0.070	0.046	0.035	0.044 \pm 0.021
Ridge	0.010	0.061	0.070	0.045	0.034	0.044 \pm 0.021
Elastic net	0.010	0.061	0.070	0.046	0.037	0.045 \pm 0.021
MCP	0.010	0.061	0.069	0.047	0.035	0.044 \pm 0.021
D/DML	0.010	0.061	0.070	0.046	0.035	0.044 \pm 0.021
NFR	0.010	0.061	0.071	0.042	0.033	0.044 \pm 0.021
DML						
Lasso	0.012	0.064	0.086	0.020	0.006	0.038 \pm 0.032
Ridge	0.010	0.063	0.068	0.024	0.005	0.034 \pm 0.027
Elastic net	0.012	0.064	0.085	0.020	0.006	0.038 \pm 0.032
MCP	0.010	0.063	0.068	0.024	0.005	0.034 \pm 0.027
D/DML	0.010	0.063	0.071	0.025	0.013	0.037 \pm 0.026
NFR	0.010	0.062	0.067	0.025	0.003	0.034 \pm 0.026

The IPW results are similar because the same classifier (random forest) is used to get the propensity scores.

Baselines In our experiment, we consider two aspects of potential baseline methods. The first aspect is from the statistical field, where approaches such as those presented in Lin et al. (2023) assume a linear relationship between the functional output and the scalar input. They utilize regularization techniques like lasso, ridge, and elastic net to estimate the causal effect map. Additionally, Chen et al. (2016) addresses situations with a large number of covariates by using the group minimax concave penalty (MCP) for variable selection and fitting. However, these methods inherently assume a linear form between the functional output and scalar input, possibly overlooking the presence of nonlinear relationships in the data. The second aspect is from the deep learning field, where we compare our model with classical Double/debiased machine learning (D/DML) proposed in Chernozhukov et al. (2018). This approach introduces a DML estimator to investigate the causal impact of scalar input on scalar outcome. To model the functional outcome, we conduct independent regressions at interesting quantiles using a standard MLP. Subsequently, we concatenate all the quantile counterfactuals to form a distribution.

Experiment Setting The classification and functional regression models are trained separately. 5,000 generated instances are trained using 5-fold cross-fitting, i.e., 4,000 instances are used to train, and 1,000 instances are used to obtain the three estimators (i.e., DR, IPW, and DML estimator). At last, we average the obtained estimators from the 5 folds as the final results. In the classification task, we use the same classifier (i.e., random forest) to compute IPW for all the estimators. The training details are given in Appendix E.

Evaluation Metric Since $\mathcal{L}(\theta, \{\gamma_{ij}\})$ in (13) is continuous, we discretize it and compare the mean absolute error (MAE) between true causal effect map $\Delta_{d^{ij}} (1 \leq i, j \leq 5)$ (computed from Eqns. (14a) - (14b)) and estimated causal effect map $\hat{\Delta}_{d^{ij}}$ on 5 quantiles with levels ranging from 10% to 90%. We repeat the experiment 50 times to report the mean and standard deviation of MAE.

Experiment Results Table 2 presents a summary of the experiment results. We observe several key findings: Firstly, NFR Net demonstrates superior performance compared to all statistical models, particularly on the DR methods. This result can be attributed to the capability of our proposed model to capture non-linear patterns between covariates and the outcome distribution effectively. Secondly, NFR Net outperforms the D/DML method. The advantage stems from our ability to model the outcome as a function. In contrast, D/DML treats each quantile as independent scalar points, overlooking the continuous structure of the distribution. Lastly, DML can utilize the IPW estimator to correct most of the bias in the DR estimator, and the DML estimator demonstrates improved robustness compared to both the DR and IPW estimators.

5 Empirical Experiment

E-commerce platforms face a significant challenge in comprehending the impact of credit lines on consumer spending patterns, particularly in terms of the shift in spending distribution caused by changes in the credit lines. To address this issue, we employ our approach by leveraging data collected from a large e-commerce platform. The platform assigns distinct credit lines to users based on various factors such as income, age, and past behaviors like shopping and default behaviors. Besides, the platform provides users with an interest-free, one-month loan option for their purchases, with the condition that the total loan amount must not exceed their assigned credit lines.

We collect data from 4,043 platform users. The data comprises various variables, such as demographic information (e.g., age, income, and location), purchasing behaviors (e.g., the total number of orders, the amount paid for each order), and financial information (e.g., credit lines assigned by the platform, the total number of loans, and the presence of default records). Appendix F displays a detailed statistical description. All the paid amounts of orders constitute a unique spending distribution for each user (e.g., Figure 7). In our empirical study, we investigate the causal maps when the credit lines take values as Low (from 0 to 9,000), Middle (from 9,000 to 15,000), and High (higher than 15,000).

Table 3: The results of the causal map of three treatments at 9 quantiles (mean and 95% CI).

Quantiles	Low	Middle	High	Low→Middle	Low→High
10%	28.0 (27.8, 28.3)	29.9 (29.8, 30.0)	30.6 (30, 31.2)	6.79%↑	9.29%↑
20%	43.6 (43.4, 43.9)	47.4 (47.1, 47.8)	48.8 (47.9, 49.5)	8.72%↑	11.93%↑
30%	58.7 (58.3, 59.0)	65.5 (65.1, 65.9)	67.5 (66.5, 68.4)	11.58%↑	14.99%↑
40%	75.2 (74.7, 75.6)	86.8 (86.3, 87.2)	91.0 (90.0, 92.1)	15.43%↑	21.01%↑
50%	94.9 (94.3, 95.6)	115.8 (114.9, 116.9)	122.4 (121.1, 123.8)	22.02%↑	28.98%↑
60%	119.0 (118.2, 119.7)	150.8 (149.7, 152.0)	170.8 (167.4, 174.7)	26.72%↑	43.53%↑
70%	155.1 (153.7, 156.4)	207.0 (205.6, 208.5)	256.0 (251.8, 261.5)	33.46%↑	65.05%↑
80%	212.9 (210.8, 214.6)	325.6 (323.2, 328.3)	433.0 (424.4, 442.7)	52.94%↑	103.38%↑
90%	381.0 (374.1, 386.7)	654.5 (650.7, 658.4)	1020.3 (1003.8, 1036.9)	71.78%↑	167.80%↑

In Table 3, we give 9 percentiles of the causal map Δ_{High} , Δ_{Middle} , and Δ_{Low} of all the consumers' spending distributions if they are assigned to High, Middle, and Low credit lines, respectively. Generally, the lower quantile of spending distribution stands for life necessities, while the higher quantiles represent luxury goods. Our findings support prior research (Aydin, 2022; Soman and Cheema, 2002), revealing a positive correlation between credit lines and spending since the causal effect maps $\Delta_{High} - \Delta_{Low}$ and $\Delta_{Middle} - \Delta_{Low}$ are always positive at all quantiles. Additionally, we observe that such an effect is heterogeneous across different quantiles. Specifically, when the credit lines increase, the spending on higher quantiles (e.g., higher than 70%) grows significantly while the spending on lower quantiles increases relatively slowly. For example, when credit lines change from Low to High, the spending at 90% quantile increases from 381.0 to 1020.3 (increasing about 167.8%) while the spending at 10% quantile only increases from 28.0 to 30.6 (increasing

about 9.3%). This suggests that users tend to increase their spending on luxury goods or services when they are able to access higher credit.

6 Conclusion

We study the causal inference on distributional outcomes with multiple treatments in the Wasserstein space. Our target quantity, the causal effect map, is the analogy to ATE in classical causal inference literature. We then propose three estimators, i.e., DR, IPW, and DML estimators, and study their asymptotic properties. Our proposed NFR Net captures complex patterns among covariates, treatments, and functional outcomes, which is verified by the synthetic experiment. Moreover, we apply it to a credit dataset and explore the causal relationship between credit lines and spending distributions. We find that when credit lines increase, the spending at every quantile level increases, with a more significant change at higher quantiles.

Generally, the credit lines is measured continuously, and a potential future research direction involves investigating causal inference in the context of continuous treatment. Additionally, the realized distribution can be multivariate, such as the joint distribution of spending behavior and credit risk, providing an opportunity to explore such scenarios.

7 Acknowledgments

Qi Wu acknowledges the support from The CityU-JD Digits Joint Laboratory in Financial Technology and Engineering; The Hong Kong Research Grants Council [General Research Fund 11219420/9043008 and 11200219/9042900]; The HK Institute of Data Science. The work described in this paper was partially supported by the InnoHK initiative, The Government of the HKSAR, and the Laboratory for AI-Powered Financial Technologies.

References

- Aydin, D. (2022). Consumption response to credit expansions: Evidence from experimental assignment of 45,307 credit lines. *American Economic Review*, 112(1):1–40.
- Cai, X., Xue, L., Cao, J., and Initiative, A. D. N. (2022). Robust estimation and variable selection for function-on-scalar regression. *Canadian Journal of Statistics*, 50(1):162–179.
- Chen, Y., Goldsmith, J., and Ogden, R. T. (2016). Variable selection in function-on-scalar regression. *Stat*, 5(1):88–101.
- Chernozhukov, V., Chetverikov, D., Demirer, M., Duflo, E., Hansen, C., Newey, W., and Robins, J. (2018). Double/debiased machine learning for treatment and structural parameters. *Econometrics Journal*, 21(1).
- Chernozhukov, V. and Hansen, C. (2005). An iv model of quantile treatment effects. *Econometrica*, 73(1):245–261.
- Chib, S. and Jacobi, L. (2007). Modeling and calculating the effect of treatment at baseline from panel outcomes. *Journal of Econometrics*, 140(2):781–801.
- Ecker, K., de Luna, X., and Schelin, L. (2023). Causal inference with a functional outcome. *arXiv preprint arXiv:2304.07113*.
- Feyoux, N., Vidard, A., and Nodet, M. (2018). Optimal transport for variational data assimilation. *Nonlinear Processes in Geophysics*, 25(1):55–66.
- Guttman-Kenney, B., Firth, C., and Gathergood, J. (2023). Buy now, pay later (bnpl)... on your credit card. *Journal of Behavioral and Experimental Finance*, page 100788.

- Hirano, K., Imbens, G. W., and Ridder, G. (2003). Efficient estimation of average treatment effects using the estimated propensity score. *Econometrica*, 71(4):1161–1189.
- Horvitz, D. G. and Thompson, D. J. (1952). A generalization of sampling without replacement from a finite universe. *Journal of the American statistical Association*, 47(260):663–685.
- Huang, Y., Leung, C. H., Yan, X., Wu, Q., Peng, N., Wang, D., and Huang, Z. (2021). The causal learning of retail delinquency. *Proceedings of the AAAI Conference on Artificial Intelligence*, 35(1):204–212.
- Jacobi, L., Wagner, H., and Frühwirth-Schnatter, S. (2016). Bayesian treatment effects models with variable selection for panel outcomes with an application to earnings effects of maternity leave. *Journal of Econometrics*, 193(1):234–250.
- Lin, Z., Kong, D., and Wang, L. (2023). Causal inference on distribution functions. *Journal of the Royal Statistical Society Series B: Statistical Methodology*, 85(2):378–398.
- Machado, J. A. and Mata, J. (2005). Counterfactual decomposition of changes in wage distributions using quantile regression. *Journal of applied Econometrics*, 20(4):445–465.
- Panaretos, V. M. and Zemel, Y. (2019). Statistical aspects of wasserstein distances. *Annual review of statistics and its application*, 6:405–431.
- Panaretos, V. M. and Zemel, Y. (2020). *An invitation to statistics in Wasserstein space*. Springer Nature.
- Ramsay, J. O. and Silverman, B. W. (2005). *Fitting differential equations to functional data: Principal differential analysis*. Springer.
- Rosenbaum, P. R. and Rubin, D. B. (1983). The central role of the propensity score in observational studies for causal effects. *Biometrika*, 70(1):41–55.
- Rubin, D. B. (1977). Assignment to treatment group on the basis of a covariate. *Journal of educational Statistics*, 2(1):1–26.
- Rubin, D. B. (1978). Bayesian inference for causal effects: The role of randomization. *The Annals of statistics*, pages 34–58.
- Rubin, D. B. (2005). Causal inference using potential outcomes: Design, modeling, decisions. *Journal of the American Statistical Association*, 100(469):322–331.
- Shi, C., Blei, D., and Veitch, V. (2019). Adapting neural networks for the estimation of treatment effects. *Advances in neural information processing systems*, 32.
- Soman, D. and Cheema, A. (2002). The effect of credit on spending decisions: The role of the credit limit and credibility. *Marketing Science*, 21(1):32–53.
- Verdinelli, I. and Wasserman, L. (2019). Hybrid wasserstein distance and fast distribution clustering. *Electronic Journal of Statistics*, 13:5088–5119.
- Villani, C. (2021). *Topics in optimal transportation*, volume 58. American Mathematical Soc.
- Wang, J.-L., Chiou, J.-M., and Müller, H.-G. (2016). Functional data analysis. *Annual Review of Statistics and its application*, 3:257–295.

A Causal Assumptions

We introduce the assumptions that are used for causal inference in Section 3.1. Here, we explain the importance of each assumption.

Consistency It assures that the observed outcome is due to the assigned intervention that allows us to examine the target quantities from the observable dataset.

Ignorability/Unconfoundness It has two meanings. First, if two units have the same \mathbf{X} , then the joint distributions of $(\mathcal{Y}(d^1), \dots, \mathcal{Y}(d^r))$ conditioning on the covariates \mathbf{X} and the treatment assignment of the two units are the same. Second, the treatment assignment mechanism should be the same if two units have the same \mathbf{X} . This assumption is not stronger than the assumption for scalar outcomes since the outcome distribution should be understood as a whole part. In our context, this assumption indicates that given one's covariates, the spending behavior under different treatments is independent of the treatment assignment.

Positivity It assures that every treatment has the chance to be assigned to the units. Indeed, if the probability of a particular treatment is 0, then it is impossible to evaluate the effects due to the treatment.

Apart from the Consistency, Ignorability/Unconfoundness, and Overlap assumptions, we also assume the SUTVA assumption:

Assumption 1. *It contains two parts:*

1. *The potential outcome of a unit is not influenced by the treatment assignment to other units.*
2. *For each unit, there are no different forms of treatment levels that lead to different potential outcomes.*

Indeed, Statement (1) assures that the potential outcome of a unit is due to the treatment level that the unit receives but not the treatment assignment to other units. Statement (2) ensures that each treatment level should be clearly characterized. Concretely, consider the case that we are interested in the effects of taking Aspirin. If the treatment variable is binary (either taking Aspirin or not), then every patient who takes Aspirin should take the same type of Aspirin and dosage. No patients are allowed to take different dosages. If the dosage is essential, then the treatment should be the dosages of Aspirin a patient takes but not dichotomous.

B Causal Quantities on Distributions

We emphasize that $(\mathcal{Y}, \mathcal{Y}(d))$ and $(Y, Y(d))$ have different meanings. $(Y, Y(d))$ is the outcome variable, and its realization is scalar values, while $(\mathcal{Y}, \mathcal{Y}(d))$ is the outcome variable such that its realization is distribution. In the main paper, we give a parametric example illustrating the meaning of $(\mathcal{Y}, \mathcal{Y}(d))$. Here, we give two concrete examples illustrating the differences when the outcome is either $(Y, Y(d))$ and $(\mathcal{Y}, \mathcal{Y}(d))$.

Example 1 (When Y for each unit under treatment d^i is scalar/vector). *Suppose the potential outcome distribution is $\mathcal{N}(0, 1)$. Then Y for each unit under treatment d^i is a realization from the distribution $\mathcal{N}(0, 1)$.*

Example 2 (When \mathcal{Y} for each unit under treatment d^i is a distribution). *We give a parametric example. Denote μ and σ as the mean and standard deviation of a normal distribution. Suppose that $(\mu, \log \sigma) \sim \mathcal{N}\left(\begin{bmatrix} 0 \\ 0 \end{bmatrix}, \begin{bmatrix} 0 & 1 \\ 1 & 0 \end{bmatrix}\right)$. If one realization of $(\mu, \log \sigma)$ is $(0.1, -0.5)$, then $(\mu, \sigma^2) = (0.1, e^{-1})$. It means that for a given unit, there is a collection of observations that are drawn from $\mathcal{N}(0.1, e^{-1})$. If another realization*

of $(\mu, \log \sigma)$ is given (say $(-0.3, 1)$), it means that a new unit would have a collection of observations that are drawn from $\mathcal{N}(-0.3, e^2)$.

We further provide two examples to illustrate the differences between the ATE (average treatment effect) and the causal effect map.

Example 3 (When Y for each unit under treatment d^i is scalar/vector). Consider three units A, B, C, whose observations and potential outcomes are as follows:

Unit	$Y(0)$	$Y(1)$	$Y(1) - Y(0)$
A	2	6	4
B	1	5	4
C	3	3	0

Then, the sampled average treatment effect (ATE) = $(4+4+0)/3=8/3$. The sampled quantile treatment effect (QTE) at $\tau = 0.5 = \text{median of } Y(1) - \text{median of } Y(0) = 5 - 2 = 3$.

Example 4 (When \mathcal{Y} for each unit under treatment d^i is a distribution). Consider three units A, B, C, whose observations can be constituted as distributions (e.g., $[2, 0, 1] \sim \mathcal{N}(1, 1)$), respectively. The potential outcomes are as follows:

Unit	$\mathcal{Y}(0)$	$\mathcal{Y}(1)$
A	$[2, 0, 1] \sim \mathcal{N}(1, 1)$	$[6] \sim \mathcal{N}(5, 1)$
B	$[1, 3, 5] \sim \mathcal{N}(3, 1)$	$[5, 10] \sim \mathcal{N}(8, 1)$
C	$[3, 4, 5] \sim \mathcal{N}(4, 1)$	$[3, 6, 6, 6] \sim \mathcal{N}(6, 1)$

Note that for normal distributions with the same variance, the Wasserstein barycenter for these distributions is also normal distribution, with its mean equal to the averaged mean of these distributions since the Wasserstein barycenter is the distribution that has the smallest Wasserstein distance of these distributions. For example, the Wasserstein barycenter for $\mathcal{N}(a, s^2)$, $\mathcal{N}(b, s^2)$, $\mathcal{N}(c, s^2)$ is $\mathcal{N}\left(\frac{a+b+c}{3}, s^2\right)$ with the following CDF:

$$\int_{-\infty}^x \frac{1}{\sqrt{2\pi}s} \exp\left(-\frac{(z - \frac{a+b+c}{3})^2}{2s^2}\right) dz.$$

Thus, in this example, the sampled barycenter for $\mathcal{Y}(0)$ is

$$\text{Erf}(x) = \int_{-\infty}^x \frac{1}{\sqrt{2\pi}} \exp\left(-\frac{(z - \frac{8}{3})^2}{2}\right) dz$$

and the sampled barycenter for $\mathcal{Y}(1)$ is

$$\text{Erf}(x) = \int_{-\infty}^x \frac{1}{\sqrt{2\pi}} \exp\left(-\frac{(z - \frac{19}{3})^2}{2}\right) dz.$$

Thus, the causal effect map between $\mathcal{Y}(0)$ and $\mathcal{Y}(1)$ is

$$\text{Erf}^{-1}(x) - \text{Erf}^{-1}(x).$$

Note that in real cases, the distributions for each unit are more complex than the normal distribution, and they even may not follow any known distributions.

C Consistency of DR and IPW estimators

In this section, we are going to study the asymptotic properties of the DR and IPW estimators. The studies require the following Lemmas:

Lemma 1. Let $m_{d^i}(\mathbf{X}) = \mathbb{E}[\mathcal{Y}^{-1}|D = d^i, \mathbf{X}]$. We have

$$\Delta_{d^i}(\cdot) = \mathbb{E}[m_{d^i}(\mathbf{X})]$$

Proof. See the proof of Assertion 2 in the proof of Proposition 1. □

Lemma 2. Let $\pi_{d^i}(\mathbf{X}) = \mathbb{P}\{D = d^i|\mathbf{X}\}$. We have

$$\Delta_{d^i}(\cdot) = \mathbb{E}\left[\frac{\mathbf{1}_{\{D=d^i\}}}{\pi_{d^i}(\mathbf{X})}\mathcal{Y}^{-1}\right]$$

Proof. From the proof of Assertion 1 in the proof of Proposition 1, we notice that $\Delta_{d^i}(\cdot) = \mathbb{E}[\mathcal{Y}(d^i)^{-1}]$. We only need to show that

$$\mathbb{E}[\mathcal{Y}(d^i)^{-1}] = \mathbb{E}\left[\frac{\mathbf{1}_{\{D=d^i\}}}{\pi_{d^i}(\mathbf{X})}\mathcal{Y}^{-1}\right].$$

Now, we have

$$\begin{aligned} & \mathbb{E}\left[\frac{\mathbf{1}_{\{D=d^i\}}}{\pi_{d^i}(\mathbf{X})}\mathcal{Y}^{-1}\right] = \mathbb{E}\left[\mathbb{E}\left[\frac{\mathbf{1}_{\{D=d^i\}}}{\pi_{d^i}(\mathbf{X})}\mathcal{Y}^{-1}|\mathbf{X}\right]\right] \\ &= \mathbb{E}\left[\frac{1}{\pi_{d^i}(\mathbf{X})}\mathbb{E}\left[\mathbf{1}_{\{D=d^i\}}\mathcal{Y}^{-1}|\mathbf{X}\right]\right] \\ &= \mathbb{E}\left[\frac{1}{\pi_{d^i}(\mathbf{X})}\sum_{1 \leq j \leq r} \mathbb{E}[\mathbf{1}_{\{D=d^i\}}\mathcal{Y}^{-1}|D = d^j, \mathbf{X}]\mathbb{P}\{D = d^j|\mathbf{X}\}\right] \\ &= \mathbb{E}\left[\frac{1}{\pi_{d^i}(\mathbf{X})}\mathbb{E}[\mathcal{Y}^{-1}|D = d^i, \mathbf{X}]\mathbb{P}\{D = d^i|\mathbf{X}\}\right] \\ &= \mathbb{E}[\mathbb{E}[\mathcal{Y}^{-1}|D = d^i, \mathbf{X}]] \\ &\stackrel{*}{=} \mathbb{E}[\mathbb{E}[\mathcal{Y}(d^i)^{-1}|D = d^i, \mathbf{X}]] \stackrel{\star}{=} \mathbb{E}[\mathbb{E}[\mathcal{Y}(d^i)^{-1}|\mathbf{X}]] \\ &= \mathbb{E}[\mathcal{Y}(d^i)^{-1}]. \end{aligned}$$

Here, * follows from Consistency Assumption, and \star follows from Ignorability Assumption. □

From Lemmas 1 and 2, we can study the asymptotic properties of $\hat{\Delta}_{d^i;DR}$ and $\hat{\Delta}_{d^i;IPW}$. Recall the estimators $\hat{\Delta}_{d^i;DR}$ and $\hat{\Delta}_{d^i;IPW}$ here:

DR estimator $\hat{\Delta}_{d^i;DR}$:

$$\hat{\Delta}_{d^i;DR} = \sum_{k=1}^K \frac{N_k}{N} \frac{1}{N_k} \sum_{s \in \mathcal{D}_k} \hat{m}_{d^i}^k(\mathbf{X}_s). \quad (15)$$

IPW estimator $\hat{\Delta}_{d^i;IPW}$:

$$\hat{\Delta}_{d^i;IPW} = \sum_{k=1}^K \frac{N_k}{N} \frac{1}{N_k} \sum_{s \in \mathcal{D}_k} \frac{\mathbf{1}_{\{D_s=d^i\}}}{\hat{\pi}_{d^i}^k(\mathbf{X}_s)} \mathcal{Y}_s^{-1}. \quad (16)$$

We first study the asymptotic property of $\hat{\Delta}_{d^i;DR}$. Write

$$\begin{aligned}\hat{\Delta}_{d^i;DR} &= \sum_{k=1}^K \frac{N_k}{N} \frac{1}{N_k} \sum_{s \in \mathcal{D}_k} \hat{m}_{d^i}^k(\mathbf{X}_s) \\ &= \underbrace{\sum_{k=1}^K \frac{N_k}{N} \frac{1}{N_k} \sum_{s \in \mathcal{D}_k} [\hat{m}_{d^i}^k(\mathbf{X}_s) - m_{d^i}(\mathbf{X}_s)]}_{\text{I}} + \underbrace{\sum_{k=1}^K \frac{N_k}{N} \frac{1}{N_k} \sum_{s \in \mathcal{D}_k} m_{d^i}(\mathbf{X}_s)}_{\text{II}}.\end{aligned}$$

II is the sample averaging of $\mathbb{E}[m_{d^i}(\mathbf{X})]$, so II converges to $\mathbb{E}[m_{d^i}(\mathbf{X})]$ in probability. By Lemma 1, II converges to $\Delta_{d^i}(\cdot)$ in probability. Hence, the consistency of the estimator $\hat{\Delta}_{d^i;DR}$ depends on the convergence of $\hat{m}_{d^i}^k(\mathbf{X}_s)$ on $m_{d^i}(\mathbf{X}_s)$.

We then study the asymptotic property of $\hat{\Delta}_{d^i;IPW}$. Similarly, we can write

$$\begin{aligned}\hat{\Delta}_{d^i;IPW} &= \sum_{k=1}^K \frac{N_k}{N} \frac{1}{N_k} \sum_{s \in \mathcal{D}_k} \frac{\mathbf{1}_{\{D_s=d^i\}}}{\hat{\pi}_{d^i}^k(\mathbf{X}_s)} \mathcal{Y}_s^{-1} \\ &= \underbrace{\sum_{k=1}^K \frac{N_k}{N} \frac{1}{N_k} \sum_{s \in \mathcal{D}_k} \left[\frac{1}{\hat{\pi}_{d^i}^k(\mathbf{X}_s)} - \frac{1}{\pi_{d^i}(\mathbf{X}_s)} \right] \mathbf{1}_{\{D_s=d^i\}} \mathcal{Y}_s^{-1}}_{\text{I}} + \underbrace{\sum_{k=1}^K \frac{N_k}{N} \frac{1}{N_k} \sum_{s \in \mathcal{D}_k} \frac{\mathbf{1}_{\{D_s=d^i\}}}{\pi_{d^i}(\mathbf{X}_s)} \mathcal{Y}_s^{-1}}_{\text{II}}.\end{aligned}$$

Again, II is the sample averaging of $\mathbb{E}\left[\frac{\mathbf{1}_{\{D=d^i\}}}{\pi_{d^i}(\mathbf{X})} \mathcal{Y}^{-1}\right]$, so II converges to $\mathbb{E}\left[\frac{\mathbf{1}_{\{D=d^i\}}}{\pi_{d^i}(\mathbf{X})} \mathcal{Y}^{-1}\right]$ in probability. By Lemma 2, II converges to $\Delta_{d^i}(\cdot)$ in probability. Hence, the consistency of the estimator $\hat{\Delta}_{d^i;DR}$ depends on the convergence of $\hat{\pi}_{d^i}^k(\mathbf{X}_s)$ on $\pi_{d^i}(\mathbf{X}_s)$.

D Missing Proofs

D.1 Proof of Proposition 1

Proof of Proposition 1. Proof of Assertion 1: If we can prove that $\mathbb{E}[\mathcal{Y}(d^i)^{-1}] = \mu_{d^i}^{-1}$, then we have $\Delta_{d^i} = \mu_{d^i}^{-1} = \mathbb{E}[\mathcal{Y}(d^i)^{-1}]$. Let \mathcal{Q} be the set containing all the left-continuous non-decreasing functions on $(0, 1)$. If we view \mathcal{Q} as a subspace of $L^2([0, 1])$, then it is isometric to $\mathcal{W}_2(\mathcal{I})$ (Panaretos and Zemel, 2020). Indeed, $\mu_{d^i} = \arg \min_{\nu \in \mathcal{W}_2(\mathcal{I})} \mathbb{E}[\mathbb{D}_2(\mathcal{Y}(d^i), \nu)^2] \stackrel{\bullet}{=} \arg \min_{\nu \in \mathcal{Q}} \mathbb{E}[\int_0^1 |\mathcal{Y}(d^i)^{-1}(t) - \nu^{-1}(t)|^2 dt]$. Here, $\stackrel{\bullet}{=}$ follows

from Theorem 2.18 of Villani (2021). Since we can interchange the integral sign \int and \mathbb{E} , we notice that $\mathbb{E}[\int_0^1 |\mathcal{Y}(d^i)^{-1}(t) - \nu^{-1}(t)|^2 dt] = \int_0^1 \mathbb{E}[|\mathcal{Y}(d^i)^{-1}(t) - \nu^{-1}(t)|^2] dt = \int_0^1 (\mathbb{E}[\mathcal{Y}(d^i)^{-1}(t)] - \nu^{-1}(t))^2 dt + \int_0^1 \mathbb{E}[(\mathbb{E}[\mathcal{Y}(d^i)^{-1}(t)] - \mathcal{Y}(d^i)^{-1}(t))^2] dt$, and $\mathbb{E}[\int_0^1 |\mathcal{Y}(d^i)^{-1}(t) - \nu^{-1}(t)|^2 dt]$ attains its minimum when $\nu^{-1}(t) = \mathbb{E}[\mathcal{Y}(d^i)^{-1}(t)]$. We can therefore conclude that $\mu_{d^i} = (\mathbb{E}[\mathcal{Y}(d^i)^{-1}(t)])^{-1}$.

Proof of Assertion 2: From Proposition 1, $\Delta_{d^i}(\cdot) = \mathbb{E}[\mathcal{Y}(d^i)^{-1}]$. Consistency assumption assures that $\mathcal{Y}^{-1} = \mathcal{Y}(d^i)^{-1}$ since $\mathcal{Y} = \mathcal{Y}(d^i)$ when $D = d^i$. Consequently, we have $\mathbb{E}[\mathcal{Y}(d^i)^{-1}] = \mathbb{E}[\mathbb{E}[\mathcal{Y}(d^i)^{-1} | \mathbf{X}]] \stackrel{*}{=} \mathbb{E}[\mathbb{E}[\mathcal{Y}(d^i)^{-1} | D = d^i, \mathbf{X}]] \stackrel{*}{=} \mathbb{E}[\mathbb{E}[\mathcal{Y}^{-1} | D = d^i, \mathbf{X}]]$. \ast follows from Ignorability Assumption while \star follows from Consistency Assumption. Thus, we conclude that $\Delta_{d^i}(\cdot)$ is identified. \square

Before starting the proof of Theorem 1, we introduce some notations that are useful in the proof of Theorem 1.

We put a $\hat{\cdot}$ on top of a random variable which represents the estimate of the random variable. For example, we use $\hat{\mathcal{Y}}$ and $\hat{\pi}_{d^i}$ to represent the estimate of \mathcal{Y} and π_{d^i} . Since we split the observed data into K disjoint union sets $\mathcal{D}_1, \dots, \mathcal{D}_K$, we also use $\hat{\pi}_{d^i}^k$ to represent the estimate π_{d^i} based on the set \mathcal{D}_{-k} and evaluate using the set \mathcal{D}_k .

We use $m_{d^i}(\mathbf{X}) = \mathbb{E}[\mathcal{Y}(d^i)^{-1}|\mathbf{X}] = \mathbb{E}[\mathcal{Y}^{-1}|D = d^i, \mathbf{X}]$. Further, denote $\tilde{m}_{d^i}^k$ as the estimate using true \mathcal{Y} based on the set \mathcal{D}_{-k} and evaluate using the set \mathcal{D}_k . Define an inner product space with inner product $\langle h_1, h_2 \rangle = \int h_1(t)h_2(t)dt$ such that $\|h\|^2 = \int h^2(t)dt$. Further, given two functions $h_1(\cdot, \mathbf{X})$ and $h_2(\cdot, \mathbf{X})$, we define $\|h_1 - h_2\|^2$ such that $\|h_1 - h_2\|^2 = \int \|h_1(\cdot, \mathbf{x}) - h_2(\cdot, \mathbf{x})\|^2 dF_{\mathbf{X}}(\mathbf{x}) = \int \int |h_1(t, \mathbf{x}) - h_2(t, \mathbf{x})|^2 dt dF_{\mathbf{X}}(\mathbf{x}) = \mathbb{E}[\|h_1 - h_2\|^2]$, where $F_{\mathbf{X}}(\mathbf{x})$ is the cumulative distribution of \mathbf{X} . Besides, let $\rho_{\pi}^4 = \mathbb{E}[\|\hat{\pi}_{d^i}(\mathbf{X}) - \pi_{d^i}(\mathbf{X})\|^4]$; $\rho_m^4 = \max\{\|\tilde{m}_{d^i} - m_{d^i}\|^4, 1 \leq i \leq r\}$. The expectation \mathbb{E} are conditional expectation conditioning on the estimated nuisance functions. We also assume that $\mathbb{E}[\|m_{d^i}(\mathbf{X})\|^4]$, $\mathbb{E}[\|\mathcal{Y}^{-1}\|^4]$, and $\mathbb{E}[\|\mathcal{Y}(d^i)^{-1}\|^4] < \infty \forall 1 \leq i \leq r$.

Next, we state the convergence assumptions which are needed in the proof of Theorem 1.

Convergence Assumption 1. *The estimates $\hat{\mathcal{Y}}_1, \dots, \hat{\mathcal{Y}}_N$ are independent of each other. Furthermore, there are two sequences of constants $\alpha_N = o(1)$ and $\nu_N = o(1)$ such that*

$$\begin{aligned} \sup_{1 \leq s \leq N} \sup_{v \in \mathcal{W}(\mathcal{I})} \mathbb{E}[\mathbb{D}_2^2(\hat{\mathcal{Y}}_s, \mathcal{Y}_s) | \mathcal{Y}_s = v] &= O(\alpha_N^2) \\ \sup_{1 \leq s \leq N} \sup_{v \in \mathcal{W}(\mathcal{I})} \mathbb{V}[\mathbb{D}_2^2(\hat{\mathcal{Y}}_s, \mathcal{Y}_s) | \mathcal{Y}_s = v] &= O(\nu_N^4). \end{aligned}$$

Convergence Assumption 2.

1. *There exists such that*

$$\mathbb{P}\{\epsilon < \hat{\pi}_{d^i}^k < 1 - \epsilon, \forall x\} = 1.$$

2. *The outcome regression and propensity score estimates converge: $\forall i \in \{1, \dots, r\}$ and $\forall 1 \leq k \leq K$, we have*

$$\sup_x \|\tilde{m}_{d^i}^k - m_{d^i}\| = o_P(1) \quad \text{and} \quad \sup_x \|\hat{\pi}_{d^i}^k - \pi_{d^i}\| = o_P(1).$$

Convergence Assumption 3. $\|\hat{m}_{d^i}^k - \tilde{m}_{d^i}^k\| = O_P(N^{-1} + \alpha_N^2 + \nu_N^2) \forall i \in \{1, \dots, r\}$ and $1 \leq k \leq K$.

Convergence Assumption 4. *There exist constants c_1 and c_2 such that $0 < c_1 \leq \frac{N_k}{N} \leq c_2 < 1$ for all N and $1 \leq k \leq K$.*

To prove Theorem 1, we require all the Convergence Assumptions. Further, we need to assume that the two sequences α_N and ν_N in Convergence Assumption 1 satisfy $\alpha_N = o(N^{-\frac{1}{2}})$ and $\nu_N = o(N^{-\frac{1}{2}})$. Note that $\alpha_N = o(N^{-\frac{1}{2}})$ and $\nu_N = o(N^{-\frac{1}{2}})$ holds imply that $\alpha_N = o(1)$ and $\nu_N = o(1)$ automatically.

D.2 Proof of Theorem 1

The proof requires two Lemmas.

Lemma 3. *For $G_1, G_2 \in \mathcal{W}_2(\mathcal{I})$, we have $\|G_1 - G_2\| = \mathbb{D}_2(G_1, G_2)$.*

Lemma 4. *Under Convergence Assumption 1, we have $\frac{1}{N} \sum_{s=1}^N \|\hat{\mathcal{Y}}_s^{-1} - \mathcal{Y}_s^{-1}\|^2 = O_P(\alpha_N^2 + \nu_N^2)$.*

The proofs of Lemmas 3 and 4 can be found in Lin et al. (2023). Now, we are ready to prove Theorem 1.

Proof of Theorem 1. In the following proof, we assume that $K = 2$. The general case is similar. For simplicity, we define four operators $\mathbb{P}_N, \mathbb{P}_{N_k}, \mathbb{E}_N$, and \mathbb{E}_{N_k} such that given a random quantity \mathcal{O} , $\mathbb{P}_N \mathcal{O} = \frac{1}{N} \sum_{s=1}^N \mathcal{O}_s$, $\mathbb{P}_{N_k} = \frac{1}{N_k} \sum_{s \in \mathcal{D}_k} \mathcal{O}_s$, $\mathbb{E}_N = \frac{1}{N} \sum_{s=1}^N \mathbb{E}[\mathcal{O}_s]$, and $\mathbb{E}_{N_k} = \frac{1}{N_k} \sum_{s \in \mathcal{D}_k} \mathbb{E}[\mathcal{O}_s]$. Given the distributions λ . Define $\mathcal{L}\lambda = \lambda^{-1}$. Let $Z_s = \mathcal{L}\mathcal{Y}_s$, and if the s^{th} subject belongs to the k partition, then $\hat{Z}_s = \mathcal{L}\hat{\mathcal{Y}}_s$ and $R_s = \hat{Z}_s - Z_s$. Define $D_{d^i}^k(x) = \hat{m}_{d^i}^k(x) - \tilde{m}_{d^i}^k(x)$. Under the causal assumptions, we have

$$\Delta_{d^i} = \mathbb{E} \left[\frac{\mathbf{1}_{\{D=d^i\}} \mathcal{L}\mathcal{Y}}{\pi_{d^i}(\mathbf{X})} - \left(\frac{\mathbf{1}_{\{D=d^i\}}}{\pi_{d^i}(\mathbf{X})} - 1 \right) m_{d^i}(\mathbf{X}) \right].$$

Denote the corresponding sampled version using \mathcal{D}_k as

$$\hat{\Delta}_{d^i; DML}^k = \mathbb{P}_{N_k} \left[\frac{\mathbf{1}_{\{D=d^i\}} \mathcal{L}\hat{\mathcal{Y}}}{\hat{\pi}_{d^i}^k(\mathbf{X})} - \left(\frac{\mathbf{1}_{\{D=d^i\}}}{\hat{\pi}_{d^i}^k(\mathbf{X})} - 1 \right) \hat{m}_{d^i}^k(\mathbf{X}) \right].$$

As a result, we have the cross-fitting estimator $\hat{\Delta}_{d^i; DML}$ such that

$$\begin{aligned} \hat{\Delta}_{d^i; DML} &= \sum_{k=1}^2 \frac{N_k}{N} \hat{\Delta}_{d^i; DML}^k \\ &= \frac{1}{N} (N_1 \hat{\Delta}_{d^i; DML}^1 + N_2 \hat{\Delta}_{d^i; DML}^2). \end{aligned}$$

Next, we consider the difference $\hat{\Delta}_{d^i; DML} - \Delta_{d^i}$. Indeed, we have

$$\frac{1}{N} (N_1 \hat{\Delta}_{d^i; DML}^1 + N_2 \hat{\Delta}_{d^i; DML}^2) - \Delta_{d^i} = \frac{1}{N} \sum_{k=1,2} N_k \mathcal{A}_k - \Delta_{d^i},$$

where

$$\mathcal{A}_k = \mathbb{P}_{N_k} \left[\frac{\mathbf{1}_{\{D=d^i\}} Z + \mathbf{1}_{\{D=d^i\}} R}{\hat{\pi}_{d^i}^k(\mathbf{X})} - \left(\frac{\mathbf{1}_{\{D=d^i\}}}{\hat{\pi}_{d^i}^k(\mathbf{X})} - 1 \right) (\tilde{m}_{d^i}^k(\mathbf{X}) + D_{d^i}^k(\mathbf{X})) \right].$$

We then decompose $\frac{1}{N} \sum_{k=1,2} N_k \mathcal{A}_k - \Delta_{d^i}$ into the sum of five quantities as follows:

$$\frac{1}{N} \sum_{k=1,2} N_k (\text{I} + \text{II} + \text{III} + \text{IV} + \text{V})$$

where

$$\begin{aligned} \text{I} &= (\mathbb{P}_{N_k} - \mathbb{E}_{N_k}) \left[\frac{\mathbf{1}_{\{D=d^i\}} (Z - \tilde{m}_{d^i}^k(\mathbf{X}))}{\hat{\pi}_{d^i}^k(\mathbf{X})} + \tilde{m}_{d^i}^k(\mathbf{X}) - \frac{\mathbf{1}_{\{D=d^i\}} (Z - m_{d^i}(\mathbf{X}))}{\pi_{d^i}(\mathbf{X})} - m_{d^i}(\mathbf{X}) \right] \\ \text{II} &= (\mathbb{P}_{N_k} - \mathbb{E}_{N_k}) \left[\frac{\mathbf{1}_{\{D=d^i\}} (Z - m_{d^i}(\mathbf{X}))}{\pi_{d^i}(\mathbf{X})} + m_{d^i}(\mathbf{X}) \right] \\ \text{III} &= \mathbb{E}_{N_k} \left[\frac{(\tilde{m}_{d^i}^k(\mathbf{X}) - m_{d^i}(\mathbf{X})) (\hat{\pi}_{d^i}^k(\mathbf{X}) - \mathbf{1}_{\{D=d^i\}})}{\hat{\pi}_{d^i}^k(\mathbf{X})} \right] \\ \text{IV} &= \mathbb{P}_{N_k} \left\{ \left(1 - \frac{\mathbf{1}_{\{D=d^i\}}}{\hat{\pi}_{d^i}^k(\mathbf{X})} \right) D_{d^i}^k(\mathbf{X}) \right\} \\ \text{V} &= \mathbb{P}_{N_k} \left\{ \frac{\mathbf{1}_{\{D=d^i\}} R}{\hat{\pi}_{d^i}^k(\mathbf{X})} \right\}. \end{aligned}$$

Proof of Theorem 1.1: The proof follows from the bounds of I - V (see more details in the sequel).

Proof of Theorem 1.2: The proof follows from the Central Limit Theorem and Slutsky's Lemma after we get the bounds of I - V.

In the sequel, we bound I - V subsequently.

Boundness of I: Let

$$\begin{aligned} G(D, \mathbf{X}, Z) &= \frac{\mathbf{1}_{\{D=d^i\}}\{Z - \tilde{m}_{d^i}^k(\mathbf{X})\}}{\hat{\pi}_{d^i}^k(\mathbf{X})} + \tilde{m}_{d^i}^k(\mathbf{X}) - m_{d^i}(\mathbf{X}) \\ H_1(D, \mathbf{X}, Z) &= \frac{\mathbf{1}_{\{D=d^i\}}Z\{\pi_{d^i}(\mathbf{X}) - \hat{\pi}_{d^i}^k(\mathbf{X})\}}{\hat{\pi}_{d^i}^k(\mathbf{X})\pi_{d^i}(\mathbf{X})} \\ H_2(D, \mathbf{X}, Z) &= \frac{\mathbf{1}_{\{D=d^i\}}\{\hat{\pi}_{d^i}^k(\mathbf{X})m_{d^i}(\mathbf{X}) - \pi_{d^i}(\mathbf{X})\tilde{m}_{d^i}^k(\mathbf{X})\}}{\hat{\pi}_{d^i}^k(\mathbf{X})\pi_{d^i}(\mathbf{X})} \\ H_3(D, \mathbf{X}, Z) &= \tilde{m}_{d^i}^k(\mathbf{X}) - m_{d^i}(\mathbf{X}) \\ H(D, \mathbf{X}, Z) &= H_1(D, \mathbf{X}, Z) + H_2(D, \mathbf{X}, Z) + H_3(D, \mathbf{X}, Z). \end{aligned}$$

We consider $\mathbb{E}[\|I\|^2]$. Note that

$$H(D, \mathbf{X}, Z) = \left[\frac{\mathbf{1}_{\{D=d^i\}}(Z - \tilde{m}_{d^i}^k(\mathbf{X}))}{\hat{\pi}_{d^i}^k(\mathbf{X})} + \tilde{m}_{d^i}^k(\mathbf{X}) - \frac{\mathbf{1}_{\{D=d^i\}}(Z - m_{d^i}(\mathbf{X}))}{\pi_{d^i}(\mathbf{X})} - m_{d^i}(\mathbf{X}) \right].$$

Hence, we have

$$\mathbb{E}[\|I\|^2] = \mathbb{E}[\|(\mathbb{P}_{N_k} - \mathbb{E}_{N_k})H(D, \mathbf{X}, Z)\|^2].$$

We simplify the quantity $\mathbb{E}[\|(\mathbb{P}_{N_k} - \mathbb{E}_{N_k})H(D, \mathbf{X}, Z)\|^2]$. Indeed, we have

$$\begin{aligned} &\mathbb{E}[\|(\mathbb{P}_{N_k} - \mathbb{E}_{N_k})H(D, \mathbf{X}, Z)\|^2] \\ &= \frac{1}{N_k^2} \mathbb{E}[\|\sum_{s \in \mathcal{D}_k} \{H(D_s, \mathbf{X}_s, Z_s) - \mathbb{E}[H(D_s, \mathbf{X}_s, Z_s)]\}\|^2] \\ &= \frac{1}{N_k^2} \sum_{s \in \mathcal{D}_k} \mathbb{E}[\|H(D_s, \mathbf{X}_s, Z_s) - \mathbb{E}[H(D_s, \mathbf{X}_s, Z_s)]\|^2] + \frac{1}{N_k^2} \sum_{\substack{s, \bar{s} \in \mathcal{D}_k \\ s \neq \bar{s}}} C_{s\bar{s}} := I_1 + I_2, \end{aligned}$$

where $C_{s\bar{s}} = \mathbb{E}[\langle H_s - \mathbb{E}[H_s], H_{\bar{s}} - \mathbb{E}[H_{\bar{s}}] \rangle]$ and $H_s = H(D_s, \mathbf{X}_s, Z_s)$. Consider the term I_1 . We have

$$\begin{aligned} I_1 &\lesssim \frac{1}{N_k^2} \sum_{s \in \mathcal{D}_k} \mathbb{E}[\|H(D_s, \mathbf{X}_s, Z_s)\|^2] \\ &\leq \frac{1}{N_k^2} \sum_{s \in \mathcal{D}_k} \mathbb{E}[\|H_1(D_s, \mathbf{X}_s, Z_s)\|^2] + \frac{1}{N_k^2} \sum_{s \in \mathcal{D}_k} \mathbb{E}[\|H_2(D_s, \mathbf{X}_s, Z_s)\|^2] + \frac{1}{N_k^2} \sum_{s \in \mathcal{D}_k} \mathbb{E}[\|H_3(D_s, \mathbf{X}_s, Z_s)\|^2]. \end{aligned}$$

Consider the bound $\mathbb{E}[\|H_1(D_s, \mathbf{X}_s, Z_s)\|^2]$, Using the assumption that there exists $\epsilon > 0$ such that $\hat{\pi}_{d^i}^k(\mathbf{X})$ and $\pi_{d^i}(\mathbf{X})$ are bounded below by $\epsilon \leq \hat{\pi}_{d^i}^k(\mathbf{X}), \pi_{d^i}(\mathbf{X}) \leq 1 - \epsilon$, we have

$$\begin{aligned} \mathbb{E}[\|H_1(D_s, \mathbf{X}_s, Z_s)\|^2] &= \mathbb{E}\left[\left\|\frac{\mathbf{1}_{\{D=d^i\}}Z\{\pi_{d^i}(\mathbf{X}) - \hat{\pi}_{d^i}^k(\mathbf{X})\}}{\hat{\pi}_{d^i}^k(\mathbf{X})\pi_{d^i}(\mathbf{X})}\right\|^2\right] \\ &\leq \mathbb{E}[\|Z\{\pi_{d^i}(\mathbf{X}) - \hat{\pi}_{d^i}^k(\mathbf{X})\}\|^2] = \mathbb{E}[|\pi_{d^i}(\mathbf{X}) - \hat{\pi}_{d^i}^k(\mathbf{X})|^2 \|Z\|^2] \\ &\leq (\mathbb{E}[|\pi_{d^i}(\mathbf{X}) - \hat{\pi}_{d^i}^k(\mathbf{X})|^4])^{\frac{1}{2}} (\mathbb{E}[\|Z\|^4])^{\frac{1}{2}} \lesssim \rho_\pi^2. \end{aligned}$$

Next, consider the bound $\mathbb{E}[\|H_2(D_s, \mathbf{X}_s, Z_s)\|^2]$. Again, using the assumption that there exists $\epsilon > 0$ such that $\hat{\pi}_{d^i}^k(\mathbf{X})$ and $\pi_{d^i}(\mathbf{X})$ are bounded below by $\epsilon \leq \hat{\pi}_{d^i}^k(\mathbf{X}), \pi_{d^i}(\mathbf{X}) \leq 1 - \epsilon$, we have

$$\begin{aligned} & \mathbb{E}[\|H_2(D_s, \mathbf{X}_s, Z_s)\|^2] \\ &= \mathbb{E}\left[\left\|\frac{\mathbf{1}_{\{D=d^i\}}\{\hat{\pi}_{d^i}^k(\mathbf{X})m_{d^i}(\mathbf{X}) - \pi_{d^i}(\mathbf{X})\tilde{m}_{d^i}^k(\mathbf{X})\}}{\hat{\pi}_{d^i}^k(\mathbf{X})\pi_{d^i}(\mathbf{X})}\right\|^2\right] \\ &\lesssim \mathbb{E}\left[\left\|\frac{\hat{\pi}_{d^i}^k(\mathbf{X})m_{d^i}(\mathbf{X}) - \pi_{d^i}(\mathbf{X})m_{d^i}(\mathbf{X})}{\hat{\pi}_{d^i}^k(\mathbf{X})\pi_{d^i}(\mathbf{X})}\right\|^2\right] + \mathbb{E}\left[\left\|\frac{\pi_{d^i}(\mathbf{X})m_{d^i}(\mathbf{X}) - \pi_{d^i}(\mathbf{X})\tilde{m}_{d^i}^k(\mathbf{X})}{\hat{\pi}_{d^i}^k(\mathbf{X})\pi_{d^i}(\mathbf{X})}\right\|^2\right] \\ &\lesssim \mathbb{E}[\|\hat{\pi}_{d^i}^k(\mathbf{X}) - \pi_{d^i}(\mathbf{X})\|^2 \|m_{d^i}(\mathbf{X})\|^2] + \mathbb{E}[\|m_{d^i}(\mathbf{X}) - \tilde{m}_{d^i}^k(\mathbf{X})\|^2] \\ &\leq (\mathbb{E}[\|\hat{\pi}_{d^i}^k(\mathbf{X}) - \pi_{d^i}(\mathbf{X})\|^4])^{\frac{1}{2}} (\mathbb{E}[\|m_{d^i}(\mathbf{X})\|^4])^{\frac{1}{2}} + \mathbb{E}[\|m_{d^i}(\mathbf{X}) - \tilde{m}_{d^i}^k(\mathbf{X})\|^2] \lesssim \rho_\pi^2 + \rho_m^2. \end{aligned}$$

Besides, we can bound $\mathbb{E}[\|H_3(D_s, \mathbf{X}_s, Z_s)\|^2]$ similarly. Indeed, we have

$$\mathbb{E}[\|H_3(D_s, \mathbf{X}_s, Z_s)\|^2] = \mathbb{E}[\|\tilde{m}_{d^i}^k(\mathbf{X}) - m_{d^i}(\mathbf{X})\|^2] \leq \rho_m^2.$$

As a result, we have

$$\mathbf{I}_1 \lesssim \frac{1}{N_k}(\rho_\pi^2 + \rho_m^2) = \frac{N}{N_k} \frac{1}{N}(\rho_\pi^2 + \rho_m^2) \lesssim \frac{1}{N}(\rho_\pi^2 + \rho_m^2).$$

We now consider the quantity \mathbf{I}_2 . Note that

$$\begin{aligned} H(D, \mathbf{X}, Z) &= \left[\frac{\mathbf{1}_{\{D=d^i\}}(Z - \tilde{m}_{d^i}^k(\mathbf{X}))}{\hat{\pi}_{d^i}^k(\mathbf{X})} + \tilde{m}_{d^i}^k(\mathbf{X}) - \frac{\mathbf{1}_{\{D=d^i\}}(Z - m_i(\mathbf{X}))}{\pi_{d^i}(\mathbf{X})} - m_{d^i}(\mathbf{X}) \right] \\ &= G(D, \mathbf{X}, Z) - \frac{\mathbf{1}_{\{D=d^i\}}(Z - m_{d^i}(\mathbf{X}))}{\pi_{d^i}(\mathbf{X})} \end{aligned}$$

and $\mathbb{E}[H(D, \mathbf{X}, Z)] = \mathbb{E}[G(D, \mathbf{X}, Z)]$. Abbreviating the notation that $G(D, \mathbf{X}, Z) = G$, since the s^{th} -unit and the \bar{s}^{th} -unit are independent of each other, we have

$$\begin{aligned} & \mathbb{E}[\langle H_s - \mathbb{E}[H_s], H_{\bar{s}} - \mathbb{E}[H_{\bar{s}}] \rangle] = \mathbb{E}[\langle G_s - \mathbb{E}[G_s], G_{\bar{s}} - \mathbb{E}[G_{\bar{s}}] \rangle] \\ &= \mathbb{E}[\langle G_s, G_{\bar{s}} \rangle] - \langle \mathbb{E}[G_s], \mathbb{E}[G_{\bar{s}}] \rangle \lesssim \|\mathbb{E}[G_s]\| \times \|\mathbb{E}[G_{\bar{s}}]\|. \end{aligned}$$

Note that

$$\begin{aligned} & \mathbb{E}[G_s] = \mathbb{E}\left[\frac{\mathbf{1}_{\{D=d^i\}}\{Z - \tilde{m}_{d^i}^k(\mathbf{X})\}}{\hat{\pi}_{d^i}^k(\mathbf{X})} + \tilde{m}_{d^i}^k(\mathbf{X}) - m_{d^i}(\mathbf{X})\right] \\ &= \mathbb{E}\left[\mathbb{E}\left[\frac{\mathbf{1}_{\{D=d^i\}}\{Z - \tilde{m}_{d^i}^k(\mathbf{X})\}}{\hat{\pi}_{d^i}^k(\mathbf{X})} \mid \mathbf{X}\right]\right] + \mathbb{E}[\tilde{m}_{d^i}^k(\mathbf{X}) - m_{d^i}(\mathbf{X})] \\ &= \mathbb{E}\left[\frac{\mathbb{E}[\mathbf{1}_{\{D=d^i\}} \mid \mathbf{X}]}{\hat{\pi}_{d^i}^k(\mathbf{X})} \{m_{d^i}(\mathbf{X}) - \tilde{m}_{d^i}^k(\mathbf{X})\}\right] + \mathbb{E}[\tilde{m}_{d^i}^k(\mathbf{X}) - m_{d^i}(\mathbf{X})] \\ &= \mathbb{E}\left[\frac{\pi_{d^i}(\mathbf{X}) - \hat{\pi}_{d^i}^k(\mathbf{X})}{\hat{\pi}_{d^i}^k(\mathbf{X})} \{m_{d^i}(\mathbf{X}) - \tilde{m}_{d^i}^k(\mathbf{X})\}\right] \\ &\lesssim \mathbb{E}[\{\pi_{d^i}(\mathbf{X}) - \hat{\pi}_{d^i}^k(\mathbf{X})\} \{m_{d^i}(\mathbf{X}) - \tilde{m}_{d^i}^k(\mathbf{X})\}]. \end{aligned}$$

Hence, we have

$$\begin{aligned} \|\mathbb{E}[G_s]\| &\lesssim \mathbb{E}[|\pi_{d^i}(\mathbf{X}) - \hat{\pi}_{d^i}^k(\mathbf{X})| \times \|m_{d^i}(\mathbf{X}) - \tilde{m}_{d^i}^k(\mathbf{X})\|] \\ &\leq (\mathbb{E}[|\pi_{d^i}(\mathbf{X}) - \hat{\pi}_{d^i}^k(\mathbf{X})|^2])^{\frac{1}{2}} (\mathbb{E}[\|m_{d^i}(\mathbf{X}) - \tilde{m}_{d^i}^k(\mathbf{X})\|^2])^{\frac{1}{2}} \\ &\leq (\mathbb{E}[|\pi_{d^i}(\mathbf{X}) - \hat{\pi}_{d^i}^k(\mathbf{X})|^4])^{\frac{1}{4}} \rho_m = \rho_\pi \rho_m. \end{aligned}$$

Hence, we have $C_{s\bar{s}} \lesssim \rho_\pi^2 \rho_m^2$ and $\mathbf{I}_2 \lesssim (1 - \frac{1}{N_k}) \rho_\pi^2 \rho_m^2$. As a result, we can show that

$$\mathbb{E}[\|\mathbf{I}\|^2] = O(N^{-1} \rho_\pi^2 + N^{-1} \rho_m^2 + \rho_\pi^2 \rho_m^2).$$

Thus, we have $I = O_P(N^{-\frac{1}{2}}\rho_\pi + N^{-\frac{1}{2}}\rho_m + \rho_\pi\rho_m)$.

Boundness of II: Note that the quantity II does not involve any estimation of nuisance functions based on the observed dataset (the function π_{d^i}) and m_{d^i} are the limits of some estimated sequences). It is equivalent to the following problem:

Claim. Given a random quantity W such that $\mathbb{E}[W] < \infty$, the sample averaging of W (i.e., $\frac{1}{N} \sum_{s=1}^N W_s$) converges to $\mathbb{E}[W]$ in probability, or $\frac{1}{N} \sum_{s=1}^N W_s - \mathbb{E}[W] = O_P\left(\frac{1}{\sqrt{N}}\right)$.

Using the Claim and Assumption 4, we have

$$\begin{aligned} \mathbb{P}\left\{\left|\frac{\text{II}}{\frac{1}{\sqrt{N}}}\right| \geq M\right\} &= \mathbb{P}\left\{\left|\frac{(\mathbb{P}_{N_k} - \mathbb{E}_{N_k})\left[\frac{\mathbf{1}_{\{D=d^i\}}(Z - m_{d^i}(\mathbf{X}))}{\pi_{d^i}(\mathbf{X})} + m_{d^i}(\mathbf{X})\right]}{\frac{1}{\sqrt{N}}}\right| \geq M\right\} \\ &\leq \frac{N}{N_k} \frac{\mathbb{E}\left[\left(\frac{\mathbf{1}_{\{D=d^i\}}(Z - m_{d^i}(\mathbf{X}))}{\pi_{d^i}(\mathbf{X})} + m_{d^i}(\mathbf{X})\right)^2\right]}{M^2}. \end{aligned}$$

We can choose sufficiently large M to make $\mathbb{P}\left\{\left|\frac{\text{II}}{\frac{1}{\sqrt{N}}}\right| \geq M\right\} < \epsilon$. Hence, we have $\text{II} = O_P(N^{-\frac{1}{2}})$.

Boundness of III: For simplicity, we denote

$$\mathcal{A} = \mathbb{E}_{N_k} \left[\frac{(\tilde{m}_{d^i}^k(\mathbf{X}) - m_{d^i}(\mathbf{X}))(\hat{\pi}_{d^i}^k(\mathbf{X}) - \mathbf{1}_{\{D=d^i\}})}{\hat{\pi}_{d^i}^k(\mathbf{X})} \right].$$

We consider the quantity $\mathbb{E}[\|\mathcal{A}\|]$. Since \mathcal{A} is an expectation already, we have $\mathbb{E}[\|\mathcal{A}\|] = \|\mathcal{A}\|$. Further, we can simplify $\|\mathcal{A}\|$ as follows:

$$\begin{aligned} \|\mathcal{A}\| &= \left\| \mathbb{E}_{N_k} \left[\frac{(\tilde{m}_{d^i}^k(\mathbf{X}) - m_{d^i}(\mathbf{X}))(\hat{\pi}_{d^i}^k(\mathbf{X}) - \mathbf{1}_{\{D=d^i\}})}{\hat{\pi}_{d^i}^k(\mathbf{X})} \right] \right\| \\ &= \left\| \mathbb{E} \left[\frac{(\tilde{m}_{d^i}^k(\mathbf{X}) - m_{d^i}(\mathbf{X}))(\hat{\pi}_{d^i}^k(\mathbf{X}) - \mathbf{1}_{\{D=d^i\}})}{\hat{\pi}_{d^i}^k(\mathbf{X})} \right] \right\| \\ &= \left\| \mathbb{E} \left[\mathbb{E} \left[\frac{(\tilde{m}_{d^i}^k(\mathbf{X}) - m_{d^i}(\mathbf{X}))(\hat{\pi}_{d^i}^k(\mathbf{X}) - \mathbf{1}_{\{D=d^i\}})}{\hat{\pi}_{d^i}^k(\mathbf{X})} \mid \mathbf{X} \right] \right] \right\| \\ &= \left\| \mathbb{E} \left[\frac{(\tilde{m}_{d^i}^k(\mathbf{X}) - m_{d^i}(\mathbf{X}))}{\hat{\pi}_{d^i}^k(\mathbf{X})} (\hat{\pi}_{d^i}^k(\mathbf{X}) - \mathbb{E}[\mathbf{1}_{\{D=d^i\}} \mid \mathbf{X}]) \right] \right\| \\ &= \left\| \mathbb{E} \left[\frac{(\tilde{m}_{d^i}^k(\mathbf{X}) - m_{d^i}(\mathbf{X}))}{\hat{\pi}_{d^i}^k(\mathbf{X})} (\hat{\pi}_{d^i}^k(\mathbf{X}) - \pi_{d^i}(\mathbf{X})) \right] \right\| \\ &\lesssim \mathbb{E}[(\tilde{m}_{d^i}^k(\mathbf{X}) - m_{d^i}(\mathbf{X}))(\hat{\pi}_{d^i}^k(\mathbf{X}) - \pi_{d^i}(\mathbf{X}))] \\ &\leq \mathbb{E}[|\hat{\pi}_{d^i}^k(\mathbf{X}) - \pi_{d^i}(\mathbf{X})|] \mathbb{E}[|\tilde{m}_{d^i}^k(\mathbf{X}) - m_{d^i}(\mathbf{X})|] \\ &\leq (\mathbb{E}[|\hat{\pi}_{d^i}^k(\mathbf{X}) - \pi_{d^i}(\mathbf{X})|^2])^{\frac{1}{2}} (\mathbb{E}[|\tilde{m}_{d^i}^k(\mathbf{X}) - m_{d^i}(\mathbf{X})|^2])^{\frac{1}{2}} \\ &\leq (\mathbb{E}[|\hat{\pi}_{d^i}^k(\mathbf{X}) - \pi_{d^i}(\mathbf{X})|^4])^{\frac{1}{4}} (\mathbb{E}[|\tilde{m}_{d^i}^k(\mathbf{X}) - m_{d^i}(\mathbf{X})|^2])^{\frac{1}{2}} \\ &\leq \rho_\pi \rho_m. \end{aligned}$$

Boundness of IV: Let $\mathcal{A} = \mathbb{P}_{N_k} \left\{ \left(1 - \frac{\mathbf{1}_{\{D=d^i\}}}{\hat{\pi}_{d^i}^k(\mathbf{X})}\right) D_{d^i}^k(\mathbf{X}) \right\}$.

Consider $\|\mathcal{A}\|^2$. We have

$$\begin{aligned} \|\mathcal{A}\|^2 &= \left\| \mathbb{P}_{N_k} \left\{ \left(1 - \frac{\mathbf{1}_{\{D=d^i\}}}{\hat{\pi}_{d^i}^k(\mathbf{X})} \right) D_{d^i}^k(\mathbf{X}) \right\} \right\|^2 \\ &= \underbrace{\frac{1}{N_k^2} \sum_{s \in \mathcal{D}^k} \left\| \left(1 - \frac{\mathbf{1}_{\{D_s=d^i\}}}{\hat{\pi}_{d^i}^k(\mathbf{X}_s)} \right) D_{d^i}^k(\mathbf{X}_s) \right\|^2}_{\text{IV}_1} + \underbrace{\frac{1}{N_k^2} \sum_{\substack{s, \bar{s} \in \mathcal{D}^k \\ s \neq \bar{s}}} \langle (1 - \frac{\mathbf{1}_{\{D_s=d^i\}}}{\hat{\pi}_{d^i}^k(\mathbf{X}_s)}) D_{d^i}^k(\mathbf{X}_s), (1 - \frac{\mathbf{1}_{\{D_{\bar{s}}=d^i\}}}{\hat{\pi}_{d^i}^k(\mathbf{X}_{\bar{s}})}) D_{d^i}^k(\mathbf{X}_{\bar{s}}) \rangle}_{\text{IV}_2}. \end{aligned}$$

Consider IV_1 first. Using Assumption 2, we see that $\text{IV}_1 \leq \frac{c}{N_k^2} \sum_{s \in \mathcal{D}^k} \|D_{d^i}^k(\mathbf{X}_s)\|^2$ for some constant c . Note that, for any $\delta > 0$, we have

$$\begin{aligned} &\mathbb{P} \left\{ \frac{1}{N_k} \sum_{s \in \mathcal{D}^k} \|D_{d^i}^k(\mathbf{X}_s)\|^2 \geq \frac{\|\hat{m}_{d^i}^k - \tilde{m}_{d^i}^k\|^2}{\delta} \right\} \\ &\leq \frac{\delta \mathbb{E} \left[\frac{1}{N_k} \sum_{s \in \mathcal{D}^k} \|D_{d^i}^k(\mathbf{X}_s)\|^2 \right]}{\|\hat{m}_{d^i}^k - \tilde{m}_{d^i}^k\|^2} = \frac{\delta \mathbb{E}[\|D_{d^i}^k(\mathbf{X})\|^2]}{\|\hat{m}_{d^i}^k - \tilde{m}_{d^i}^k\|^2} = \delta. \end{aligned}$$

Indeed, the inequality follows from Markov inequality. The last equality follows from the Definition of $\|\cdot\|^2$. According to the definition, we have $\mathbb{E}[\|D_{d^i}^k(\mathbf{X})\|^2] = \|\hat{m}_{d^i}^k - \tilde{m}_{d^i}^k\|^2$. It means that $\frac{1}{N_k} \sum_{s \in \mathcal{D}^k} \|D_{d^i}^k(\mathbf{X}_s)\|^2 = O_P(\|\hat{m}_{d^i}^k - \tilde{m}_{d^i}^k\|^2)$. Hence, we note that $\text{IV}_1 = \frac{1}{N_k} \times \frac{1}{N_k} \sum_{s \in \mathcal{D}^k} \|D_{d^i}^k(\mathbf{X}_s)\|^2 = \frac{N}{N_k} \times \frac{1}{N} \times O_P(\|\hat{m}_{d^i}^k - \tilde{m}_{d^i}^k\|^2)$.

Using Assumptions 3 and 4, we have $\text{IV}_1 = O_P(N^{-2} + N^{-1}\alpha_N^2 + N^{-1}\nu_N^2)$.

Next, we consider IV_2 . Let

$$\begin{aligned} \mathcal{A} &= (\mathbb{E}[\|D_{d^i}^k(\mathbf{X}_s)\|^4])^{\frac{1}{4}} (\mathbb{E}[\|D_{d^i}^k(\mathbf{X}_{\bar{s}})\|^4])^{\frac{1}{4}} \times \\ &\quad (\mathbb{E}[(\hat{\pi}_{d^i}^k(\mathbf{X}_s) - \pi_{d^i}(\mathbf{X}_s))^4])^{\frac{1}{4}} \mathbb{E}[(\hat{\pi}_{d^i}^k(\mathbf{X}_{\bar{s}}) - \pi_{d^i}(\mathbf{X}_{\bar{s}}))^4])^{\frac{1}{4}}. \end{aligned}$$

Note that, for any $\delta > 0$, we have

$$\begin{aligned} &\mathbb{P} \left\{ \text{IV}_2 \geq \frac{\mathcal{A}}{\delta} \right\} \\ &\leq \frac{\delta \frac{1}{N_k^2} \sum_{\substack{s, \bar{s} \in \mathcal{D}^k \\ s \neq \bar{s}}} \mathbb{E} \left[\langle (1 - \frac{\mathbf{1}_{\{D_s=d^i\}}}{\hat{\pi}_{d^i}^k(\mathbf{X}_s)}) D_{d^i}^k(\mathbf{X}_s), (1 - \frac{\mathbf{1}_{\{D_{\bar{s}}=d^i\}}}{\hat{\pi}_{d^i}^k(\mathbf{X}_{\bar{s}})}) D_{d^i}^k(\mathbf{X}_{\bar{s}}) \rangle \right]}{\mathcal{A}} \\ &\stackrel{*}{\leq} \frac{\delta \frac{1}{N_k^2} \sum_{\substack{s, \bar{s} \in \mathcal{D}^k \\ s \neq \bar{s}}} \mathcal{A}}{\mathcal{A}} = \frac{\delta N_k(N_k - 1)}{N_k^2} = \delta \left(1 - \frac{1}{N_k} \right) \leq \delta. \end{aligned}$$

Here, $\stackrel{*}{\leq}$ is due to the upper bound of the quantity $\mathbb{E}[\langle (1 - \frac{\mathbf{1}_{\{D_s=d^i\}}}{\hat{\pi}_{d^i}^k(\mathbf{X}_s)}) D_{d^i}^k(\mathbf{X}_s), (1 - \frac{\mathbf{1}_{\{D_{\bar{s}}=d^i\}}}{\hat{\pi}_{d^i}^k(\mathbf{X}_{\bar{s}})}) D_{d^i}^k(\mathbf{X}_{\bar{s}}) \rangle]$.

Indeed, using the fact that the unit s and the unit \bar{s} are independent of each other, we have

$$\begin{aligned} &\mathbb{E} \left[\langle (1 - \frac{\mathbf{1}_{\{D_s=d^i\}}}{\hat{\pi}_{d^i}^k(\mathbf{X}_s)}) D_{d^i}^k(\mathbf{X}_s), (1 - \frac{\mathbf{1}_{\{D_{\bar{s}}=d^i\}}}{\hat{\pi}_{d^i}^k(\mathbf{X}_{\bar{s}})}) D_{d^i}^k(\mathbf{X}_{\bar{s}}) \rangle \right] \\ &= \mathbb{E} \left[\left(1 - \frac{\mathbf{1}_{\{D_s=d^i\}}}{\hat{\pi}_{d^i}^k(\mathbf{X}_s)} \right) \left(1 - \frac{\mathbf{1}_{\{D_{\bar{s}}=d^i\}}}{\hat{\pi}_{d^i}^k(\mathbf{X}_{\bar{s}})} \right) \langle D_{d^i}^k(\mathbf{X}_s), D_{d^i}^k(\mathbf{X}_{\bar{s}}) \rangle \right] \\ &= \mathbb{E} \left[\langle D_{d^i}^k(\mathbf{X}_s), D_{d^i}^k(\mathbf{X}_{\bar{s}}) \rangle \mathbb{E} \left[\left(1 - \frac{\mathbf{1}_{\{D_s=d^i\}}}{\hat{\pi}_{d^i}^k(\mathbf{X}_s)} \right) \left(1 - \frac{\mathbf{1}_{\{D_{\bar{s}}=d^i\}}}{\hat{\pi}_{d^i}^k(\mathbf{X}_{\bar{s}})} \right) \middle| \mathbf{X} \right] \right] \\ &= \mathbb{E} \left[\langle D_{d^i}^k(\mathbf{X}_s), D_{d^i}^k(\mathbf{X}_{\bar{s}}) \rangle \mathbb{E} \left[\left(1 - \frac{\mathbf{1}_{\{D_s=d^i\}}}{\hat{\pi}_{d^i}^k(\mathbf{X}_s)} \right) \middle| \mathbf{X} \right] \mathbb{E} \left[\left(1 - \frac{\mathbf{1}_{\{D_{\bar{s}}=d^i\}}}{\hat{\pi}_{d^i}^k(\mathbf{X}_{\bar{s}})} \right) \middle| \mathbf{X} \right] \right]. \end{aligned}$$

Now, using Assumption 2, we can further have

$$\begin{aligned}
 & \mathbb{E} \left[\left\langle \left(1 - \frac{\mathbf{1}_{\{D_s=d^i\}}}{\hat{\pi}_{d^i}^k(\mathbf{X}_s)}\right) D_{d^i}^k(\mathbf{X}_s), \left(1 - \frac{\mathbf{1}_{\{D_{\bar{s}}=d^i\}}}{\hat{\pi}_{d^i}^k(\mathbf{X}_{\bar{s}})}\right) D_{d^i}^k(\mathbf{X}_{\bar{s}}) \right\rangle \right] \\
 & \leq \mathbb{E}[\langle D_{d^i}^k(\mathbf{X}_s), D_{d^i}^k(\mathbf{X}_{\bar{s}}) \rangle (\hat{\pi}_{d^i}^k(\mathbf{X}_s) - \pi_{d^i}(\mathbf{X}_s)) (\hat{\pi}_{d^i}^k(\mathbf{X}_{\bar{s}}) - \pi_{d^i}(\mathbf{X}_{\bar{s}}))] \\
 & \leq (\mathbb{E}[\langle D_{d^i}^k(\mathbf{X}_s), D_{d^i}^k(\mathbf{X}_{\bar{s}}) \rangle^2])^{\frac{1}{2}} \times \\
 & \quad (\mathbb{E}[(\hat{\pi}_{d^i}^k(\mathbf{X}_s) - \pi_{d^i}(\mathbf{X}_s))^2 (\hat{\pi}_{d^i}^k(\mathbf{X}_{\bar{s}}) - \pi_{d^i}(\mathbf{X}_{\bar{s}}))^2])^{\frac{1}{2}} \\
 & \leq (\mathbb{E}[\|D_{d^i}^k(\mathbf{X}_s)\|^2 \|D_{d^i}^k(\mathbf{X}_{\bar{s}})\|^2])^{\frac{1}{2}} \times \\
 & \quad (\mathbb{E}[(\hat{\pi}_{d^i}^k(\mathbf{X}_s) - \pi_{d^i}(\mathbf{X}_s))^4])^{\frac{1}{4}} \mathbb{E}[(\hat{\pi}_{d^i}^k(\mathbf{X}_{\bar{s}}) - \pi_{d^i}(\mathbf{X}_{\bar{s}}))^4])^{\frac{1}{4}} \\
 & \leq (\mathbb{E}[\|D_{d^i}^k(\mathbf{X}_s)\|^4])^{\frac{1}{4}} (\mathbb{E}[\|D_{d^i}^k(\mathbf{X}_{\bar{s}})\|^4])^{\frac{1}{4}} \\
 & \quad (\mathbb{E}[(\hat{\pi}_{d^i}^k(\mathbf{X}_s) - \pi_{d^i}(\mathbf{X}_s))^4])^{\frac{1}{4}} \mathbb{E}[(\hat{\pi}_{d^i}^k(\mathbf{X}_{\bar{s}}) - \pi_{d^i}(\mathbf{X}_{\bar{s}}))^4])^{\frac{1}{4}} \\
 & = (\mathbb{E}[\|D_{d^i}^k(\mathbf{X})\|^4])^{\frac{1}{2}} (\mathbb{E}[(\hat{\pi}_{d^i}^k(\mathbf{X}) - \pi_{d^i}(\mathbf{X}))^4])^{\frac{1}{2}} \\
 & = O_P(\rho_\pi^2 \|\hat{m}_{d^i}^k - \tilde{m}_{d^i}^k\|^2).
 \end{aligned}$$

Hence, we can conclude that $\text{IV}_2 = O_P(\rho_\pi^2 N^{-1} + \rho_\pi^2 \alpha_N^2 + \rho_\pi^2 \nu^2)$. Consequently, we obtain that $\|\text{IV}\|_\lambda^2 = O_P(N^{-2} + N^{-1} \alpha_N^2 + N^{-1} \nu_N^2 + \rho_\pi^2 N^{-1} + \rho_\pi^2 \alpha_N^2 + \rho_\pi^2 \nu^2)$, implying that $\text{IV} = O_P(N^{-1} + N^{-\frac{1}{2}} \alpha_N + N^{-\frac{1}{2}} \nu_N + \rho_\pi N^{-\frac{1}{2}} + \rho_\pi \alpha_N + \rho_\pi \nu)$.

Boundness of V: Observe that

$$\begin{aligned}
 & \mathbb{P}_{N_k} \left\{ \frac{\mathbf{1}_{\{D=d^i\}} R}{\hat{\pi}_{d^i}^k(\mathbf{X})} \right\} \\
 & = \mathbb{P}_{N_k} \left\{ \frac{\mathbf{1}_{\{D=d^i\}} R}{\pi_{d^i}(\mathbf{X})} \right\} + \mathbb{P}_{N_k} \left\{ \frac{\mathbf{1}_{\{D=d^i\}} R}{\hat{\pi}_{d^i}^k(\mathbf{X})} - \frac{\mathbf{1}_{\{D=d^i\}} R}{\pi_{d^i}(\mathbf{X})} \right\} \\
 & = \mathbb{P}_{N_k} \left\{ \frac{\mathbf{1}_{\{D=d^i\}} R}{\pi_{d^i}(\mathbf{X})} \right\} + \mathbb{P}_{N_k} \left\{ \frac{\mathbf{1}_{\{D=d^i\}} R (\pi_{d^i}(\mathbf{X}) - \hat{\pi}_{d^i}^k(\mathbf{X}))}{\hat{\pi}_{d^i}^k(\mathbf{X}) \pi_{d^i}(\mathbf{X})} \right\}.
 \end{aligned} \tag{17}$$

Using the fact that $0 < \epsilon \leq \hat{\pi}_k^i(\mathbf{X}), \pi^i(\mathbf{X}) \leq 1 - \epsilon < 1$, we have

$$\begin{aligned}
 \text{Eqn. (17)} & \lesssim \mathbb{P}_{N_k} \left\{ \frac{\mathbf{1}_{\{D=d^i\}} R}{\pi_{d^i}(\mathbf{X})} \right\} + \mathbb{P}_{N_k} \left\{ \frac{\mathbf{1}_{\{D=d^i\}} R (\pi_{d^i}(\mathbf{X}) - \hat{\pi}_{d^i}^k(\mathbf{X}))}{\pi_{d^i}(\mathbf{X})} \right\} \\
 & \leq \mathbb{P}_{N_k} \left\{ \frac{\mathbf{1}_{\{D=d^i\}} R}{\pi_{d^i}(\mathbf{X})} \right\} + 2 \mathbb{P}_{N_k} \left\{ \frac{\mathbf{1}_{\{D=d^i\}} R}{\pi_{d^i}(\mathbf{X})} \right\} \\
 & = 3 \mathbb{P}_{N_k} \left\{ \frac{\mathbf{1}_{\{D=d^i\}} R}{\pi_{d^i}(\mathbf{X})} \right\}.
 \end{aligned}$$

Hence, $\mathbb{P}_{N_k} \left\{ \frac{\mathbf{1}_{\{D=d^i\}} R}{\hat{\pi}_{d^i}^k(\mathbf{X})} \right\}$ is dominated by the quantity $\mathbb{P}_{N_k} \left\{ \frac{\mathbf{1}_{\{D=d^i\}} R}{\pi_{d^i}(\mathbf{X})} \right\}$. Besides, we can rewrite

$\mathbb{P}_{N_k} \left\{ \frac{\mathbf{1}_{\{D=d^i\}} R}{\pi_{d^i}(\mathbf{X})} \right\}$ such that

$$\mathbb{P}_{N_k} \left\{ \frac{\mathbf{1}_{\{D=d^i\}} R}{\pi_{d^i}(\mathbf{X})} \right\} = \mathbb{P}_{N_k} \left\{ \frac{\mathbf{1}_{\{D=d^i\}} (\mathcal{L}\hat{\mathcal{Y}} - \mathcal{L}\mathcal{Y})}{\pi_{d^i}(\mathbf{X})} \right\}.$$

By Lemma 4 and the assumptions of α_N and ν_N given in Convergence Assumption 1, we have $\text{V} = O_P(\alpha_N + \nu_N)$. \square

E Synthetic Experiments

E.1 Data Generation Process and Dataset Description

We simulate one synthetic dataset with non-linear causal maps and sample selection bias to test our proposed framework. The data-generating process (DGP) is as follows:

$$\mathcal{Y}_s(D_s)^{-1} = c + (1 - c)(\mathbb{E}[D] + \sqrt{D_s}) \times \sum_{j=1}^{\frac{n}{2}} \frac{\exp(X_s^{2j-1} X_s^{2j})}{\sum_{k=1}^{\frac{n}{2}} \exp(X_s^{2k-1} X_s^{2k})} \mathbf{B}^{-1}(\alpha_j, \beta_j) + \epsilon_s,$$

$$D_s = \sigma \left(\frac{\exp(\gamma_w^T \mathbf{X}_s)}{\sum_{w=1}^r \exp(\gamma_w^T \mathbf{X}_s)} \right),$$

where n is an even number which indicates the number of covariates, \mathcal{Y}_s^{-1} is the inverse distribution of unit s , \mathbf{X}_s is the covariates of unit s , and D_s is the treatment of unit s . $\mathbf{B}^{-1}(\alpha, \beta)$ is the inverse cumulative distribution function (CDF) of beta distribution with the shapes' parameters α and β . σ is a function that maps the features to treatment D such that D takes five treatment levels $\{d^1, d^2, d^3, d^4, d^5\}$. c is the constant that controls the strength of the causal relationship between D and \mathcal{Y}^{-1} . ϵ is the noise that follows $N(0, 0.05)$. In our experiments, we set $n = 10$. We assume that $X^1, X^2 \sim \mathcal{N}(-2, 1)$, $X^3, X^4 \sim \mathcal{N}(-1, 1)$, $X^5, X^6 \sim \mathcal{N}(0, 1)$, $X^7, X^8 \sim \mathcal{N}(1, 1)$, $X^9, X^{10} \sim \mathcal{N}(2, 1)$. 5 inverse beta CDFs are needed, and we set each beta distribution with different parameters to ensure the complexity of the distribution function. For each unit s , 100 observations are sampled from inverse CDF using the inverse transform sampling method. In one experiment, 5,000 instances are generated.

E.2 Training Details

The hyperparameters are tuned using the random search for both models, and we set the hyperparameters as follows: learning rate: 0.003, batch size: 128, number of epochs: 150, dropout: 0.1, weight decay: 0.001. We use Adam as the optimizer. The adaptive learning rate is used for training, and if the test accuracy does not decrease for 10 epochs, the learning rate will decrease by half.

F Empirical Experiments

Our data is collected from a large E-commerce platform that introduced the ‘‘Buy now, pay later’’ (BNPL) credit service to boost the spending of consumers. The objective of our study was to examine the impact of changes in credit lines on spending distribution. We collect data from 4,043 users on the platform over a period of 24 months, from January 2018 to December 2019. The data included demographic information such as gender, age, and location, as well as shopping behaviors such as the amount paid for each order, the total number of orders, and financial information such as the presence of default records, the total number of loans, and the credit line assigned by the platform. To eliminate the impact of the two promotion seasons in June and November, we selected July, August, September, and October of 2019 as our target research period. All the paid amounts of each order by each user during this period constitute a spending distribution for each user.

The statistical descriptions of the aforementioned features are presented in Table 4. Specifically, the average age of users in our data is 35, the number of males accounts for 59.8%, and the number of females accounts for 41.2%. The mean age of the users in our data was found to be 35, with 59.8% being male and 41.2% being

Table 4: The statistical description of training features.

	mean	std	min	25%	50%	75%	max
Age	35.211	7.272	21	30	34	39	60
Gender	0.598	0.490	0	0	1	1	1
Num of orders	209.801	108.096	78	147	180	232	2187
Default rate	0.357	0.479	0	0	0	1	1
Credit Line	10190.840	4516.421	0	7342	10000	11707	51792
$Q = 10\%$	24.467	21.315	0	6	23.61	35.934	182.98
$Q = 20\%$	41.589	33.711	0	14.88	39	59.97	779
$Q = 30\%$	60.316	76.464	0	27.97	57.4	88.952	3999
$Q = 40\%$	80.459	94.739	0	43.979	80.722	104.151	4799
$Q = 50\%$	105.422	120.121	0	63.995	99.93	126.665	4998.99
$Q = 60\%$	139.409	161.367	0	90.767	119.24	162.587	5298
$Q = 70\%$	195.481	258.942	0	105.926	155	215.935	7364
$Q = 80\%$	298.639	415.584	0	147.824	211.64	315.036	8380
$Q = 90\%$	588.585	827.340	0	237.13	365.12	599.442	15320

female. Additionally, the mean number of orders was 210, indicating a relatively high level of activity among the users in our sample. The presence of default records in 35.7% of the users highlights the need to consider financial stability. Additionally, with respect to the spending distribution, the mean of the distribution, computed from quantiles 0.1 to 0.9, varies from 24.467 to 588.585. The large variance of spending at each quantile highlights the substantial variability of the distribution of consumption among users, demonstrating the diversity of spending patterns among the individuals in the sample.

The hyperparameters are tuned using random searching for both models. We set the hyperparameters as follows: learning rate: 0.005, batch size: 128, number of epochs: 150, dropout: 0.1, weight decay: 0.001. We use Adam as the optimizer. The adaptive learning rate is used for training, and if the test accuracy does not decrease for 10 epochs, the learning rate will decrease by half. Here, we give the specific values in Table 5. Generally, the lower quantile stands for some small amount of spending, such as life necessities, while the higher quantiles represent the larger amount of spending, such as luxury goods or services.

Consistent with prior research, our findings indicate a positive correlation between credit lines and spending, highlighting the stimulating impact of credit on consumption. Additionally, we find that such an effect is heterogeneous across different quantiles. Specifically, when the credit lines increase (e.g., from Low to Middle or from Middle to High), the spending on higher quantiles grows significantly (e.g., increase from 801.57 to 1217.40 or from 1217.40 to 1770.66 at quantile 95%) while the spending on lower quantiles increases relatively slowly (e.g., increase from 19.94 to 21.27 or from 21.27 to 21.96). This suggests that users tend to increase their spending on luxury goods or services when they are able to access credit.

G G. Computation Infrastructure

All experiments are run on Dell 7920 with Intel(R) Xeon(R) Gold 6250 CPU at 3.90GHz, and a set of NVIDIA Quadro RTX 6000 GP. All models are implemented in Python 3.8. The versions of the main packages of our code are Pytorch 1.8.1+cu102, Sklearn: 0.23.2, Numpy: 1.19.2, Pandas: 1.1.3, Matplotlib: 3.3.2.

Table 5: The results of the empirical experiment.

Quantiles	Low (0-9,000)	Middle (9,000-15,000)	High (>15,000)
5%	19.9 (19.6, 20.3)	21.3 (21.1, 21.4)	22.0 (21.2, 22.7)
10%	28.0 (27.8, 28.3)	29.9 (29.8, 30.0)	30.6 (30.0, 31.2)
15%	35.4 (35.1, 35.7)	37.4 (37.3, 37.6)	39.2 (38.6, 39.9)
20%	43.6 (43.4, 43.9)	47.4 (47.1, 47.8)	48.8 (47.9, 49.5)
25%	51.2 (50.9, 51.6)	57.2 (56.8, 57.5)	57.8 (56.9, 58.5)
30%	58.7 (58.3, 59.0)	65.5 (65.1, 65.9)	67.5 (66.5, 68.4)
35%	66.6 (66.2, 67.1)	75.7 (75.3, 76.1)	78.1 (77.0, 79.0)
40%	75.2 (74.7, 75.6)	86.8 (86.3, 87.2)	91.0 (90.0, 92.1)
45%	83.9 (83.4, 84.5)	99.6 (98.8, 100.5)	104.3 (103.3, 105.4)
50%	94.9 (94.3, 95.6)	115.8 (114.9, 116.9)	122.4 (121.1, 123.8)
55%	105.6 (104.9, 106.2)	131.1 (130.0, 132.2)	142.8 (140.6, 145.4)
60%	119.0 (118.2, 119.7)	150.8 (149.7, 152.0)	170.8 (167.4, 174.7)
65%	134.8 (133.8, 135.7)	174.0 (172.7, 175.3)	206.3 (202.3, 210.9)
70%	155.1 (153.7, 156.4)	207.0 (205.6, 208.5)	256.0 (251.8, 261.5)
75%	180.7 (178.8, 182.2)	259.0 (256.9, 261.1)	327.4 (321.5, 334.5)
80%	212.9 (210.8, 214.6)	325.6 (323.2, 328.3)	433.0 (424.4, 442.7)
85%	264.1 (260.3, 266.9)	434.4 (431.4, 437.7)	615.5 (605.7, 628.6)
90%	381.0 (374.1, 386.7)	654.5 (650.7, 658.4)	1020.3 (1003.8, 1036.9)
95%	801.6 (784.5, 817.2)	1217.4 (1211.2, 1225.0)	1770.7 (1731.5, 1803.3)